OECD DOCUMENTS

Review of Nuclear Fuel Experimental Data

Fuel Behaviour Data Available from
IFE-OCDE Halden Project
for Development and Validation of Computer Codes

prepared by
James Anthony Turnbull

January 1995

NUCLEAR ENERGY AGENCY
ORGANISATION FOR ECONOMIC CO-OPERATION AND DEVELOPMENT

ORGANISATION FOR ECONOMIC CO-OPERATION AND DEVELOPMENT

Pursuant to Article 1 of the Convention signed in Paris on 14th December 1960, and which came into force on 30th September 1961, the Organisation for Economic Co-operation and Development (OECD) shall promote policies designed:

- to achieve the highest sustainable economic growth and employment and a rising standard of living in Member countries, while maintaining financial stability, and thus to contribute to the development of the world economy;
- to contribute to sound economic expansion in Member as well as non-member countries in the process of economic development; and
- to contribute to the expansion of world trade on a multilateral, non-discriminatory basis in accordance with international obligations.

The original Member countries of the OECD are Austria, Belgium,Canada, Denmark, France, Germany, Greece, Iceland, Ireland, Italy, Luxembourg, the Netherlands, Norway, Portugal, Spain, Sweden, Switzerland, Turkey, the United Kingdom and the United States. The following countries became Members subsequently through accession at the dates indicated hereafter: Japan (28th April 1964), Finland (28th January 1969), Australia (7th June 1971), New Zealand (29th May 1973) and Mexico (18th May 1994). The Commission of the European Communities takes part in the work of the OECD (Article 13 of the OECD Convention).

NUCLEAR ENERGY AGENCY

The OECD Nuclear Energy Agency (NEA) was established on 1st February 1958 under the name of the OEEC European Nuclear Energy Agency. It received its present designation on 20th April 1972, when Japan became its first non-European full Member. NEA membership today consists of all European Member countries of OECD as well as Australia, Canada, Japan, Republic of Korea, Mexico and the United States. The Commission of the European Communities takes part in the work of the Agency.

The primary objective of NEA is to promote co-operation among the governments of its participating countries in furthering the development of nuclear power as a safe, environmentally acceptable and economic energy source.

This is achieved by:

- *encouraging harmonization of national regulatory policies and practices, with particular reference to the safety of nuclear installations, protection of man against ionising radiation and preservation of the environment, radioactive waste management, and nuclear third party liability and insurance;*
- *assessing the contribution of nuclear power to the overall energy supply by keeping under review the technical and economic aspects of nuclear power growth and forecasting demand and supply for the different phases of the nuclear fuel cycle;*
- *developing exchanges of scientific and technical information particularly through participation in common services;*
- *setting up international research and development programmes and joint undertakings.*

In these and related tasks, NEA works in close collaboration with the International Atomic Energy Agency in Vienna, with which it has concluded a Co-operation Agreement, as well as with other international organisations in the nuclear field.

Credit of cover picture: Stress Corrosion Cracking in Zircaloy-4 (photo: CEA - Grenoble)

FOREWORD

This review has been carried out in the framework of activities of the OECD/NEA Task Force on Scientific Issues in Fuel Behaviour. It is published on the responsibility of the Secretary-General of the OECD. The opinions it expresses are those of the author only and do not represent the position of any Member country or international organisation.

SUMMARY

This report outlines some of the experiments that have been performed in the Halden reactor and the most important data they provided; these are available for use in fuel performance studies. It discusses in addition some experiments from the Risø fission gas release projects and the Studsvik Nuclear Ramp Programme. The report concentrates on experiments on thermal performance, fission product release, clad properties and pellet-clad mechanical interaction. Experiments where integral behaviour is measured using different types of instrumentation either within the same rod or the same irradiation assembly are highlighted. These are of particular use in code validation. As a separate topic, the report identifies experimental data relevant to high burnup behaviour.

The report recommends the preparation of an internationally available database covering as many reactor systems as possible. This would greatly assist the development of codes and mechanistic models which are preferable to those based on more restricted and specific data, as they provide more reliable predictions of fuel performance. The report also suggests that the database be structured around the topics discussed in the report. A priority list of experiments has been identified for inclusion.

Finally, the review has determined that, despite the comprehensive nature of Halden data, further experiments are required to extend the database to higher burnups, and that further measurements are necessary to investigate the time dependence of fuel temperatures during rapid over-power transients.

CONTENTS

CHAPTER 1

INTRODUCTION

In 1993, The NEA Nuclear Science Committee (NSC) set up a *Task Force on Scientific Issues of Fuel Behaviour*. During discussions at the first meeting in December 1993 it was found that there was a need for a better understanding of the underlying basic phenomena. Members were charged with the task of identifying areas of high priority which would benefit from international co-operation and to prepare a report providing advice on the developments needed in the form of experiments, data and models, to meet the requirements for a better understanding of fuel behaviour.

One of the high priority actions identified and later approved by the NSC was the setting up of an international database of well characterised experiments from different sources as a support for fuel model development and validation. As a first step it was agreed to prepare a report reviewing existing data sets and to select a subset that comprehensively covered the most important phenomena. This is the subject of this report which reviews the data available from the OECD Halden Reactor Project and touches on data available from other sources. The report also discusses the setting up of the database and the issues to be addressed in doing so.

The Need for Data

Whereas in the past, reactor operation was supported by rather simple 'scoping' calculations to ensure safety, today the requirements are much more onerous. Early bounding conditions were generous compared to normal operation, but now, with increasing emphasis on economic as well as safe operation, the approach to fuel performance is very much more detailed and closer to 'best estimate' evaluation. Not only are the safety requirements more extensive, but the economics of nuclear power production are constantly under scrutiny to ensure minimum unit cost. This is particularly the case in countries where nuclear must compete with conventional stations. For these reasons it is no longer possible to support operation with anything other than code calculations where all aspects of fuel performance are treated simultaneously and in a self consistent way. With the improvement of computer systems both in cost and speed, it is much more economic to have a small number of dedicated codes and methodologies for performance assessment than a selection of labour intensive stand alone calculations. Also, there is a move in some countries to 'shadow' operations with an on-line evaluation of fuel performance and a continuous assessment of core conditions against fixed limits for a large fraction of fuel assemblies in the reactor.

Thus the function of a fuel performance code is that it describes the behaviour of reactor fuel in the most accurate way possible under whatever conditions both normal and off-normal that are required by the licensing authority. By aiming to be a best estimate calculation or one that is intentionally biased, the uncertainties in the conditions under which the code is applied is under the control of the user.

The need for calculations to be best estimate necessitates that the code is developed and validated against good quality data. The most obvious source of these is the power reactors for which the calculations are to be applied. However, even if extensive Post Irradiation Examination (PIE) is

performed on discharged fuel, the lack of detailed information on the irradiation histories because of little or no in-pile instrumentation means that the data are of limited value. Also, data obtained this way takes a long time to obtain from the inception of the programme to the final examination. In-addition, data are needed for fuel experiencing transients and other off-normal operating conditions which cannot be reproduced under experimental conditions in a power reactor. For this reason the best quality data for code development and validation comes from well instrumented and dedicated test reactors.

There are many phenomena which are fundamental to all codes of which fuel temperatures and fission gas release are the most obvious and must represent the core of the calculations. In other areas, code requirements are country specific depending on the safety case that is supported. For example, there are requirements in Germany, France and the U.K. to perform calculations on PCI failure probability under transient over power conditions. Also, in the U.K., it is necessary to have calculations on the inventory of radioactive iodine capable of immediate escape in the event of fuel failure in coolant accidents. Thus, although the detailed requirements can be specific, there are many aspects of fuel behaviour that are common, and for economic reasons, many companies have joined International Projects and jointly funded experiments to obtain data.

CHAPTER 2

THE HALDEN REACTOR PROJECT

The OECD Halden Reactor Project is one such project. The Halden Boiling Water Reactor (HBWR) currently operated at 18 to 20 MW is situated inconspicuously within the rock on the outskirts of the town of Halden in southern Norway. The reactor has operated since 1959 and was initiated to investigate nuclear capability as a supplier of steam to the wood pulp industry.

Since that time the reactor facilities have been updated progressively and through a series of innovative techniques, the system has become one of the most versatile in the world. Over the course of this development, some 300 in-pile experiments have been performed. These ranged in complexity from rudimentary non-instrumented rod bundles to some of the most integrated and complex in-reactor tests ever designed. The Project is conducted under the auspices of the OECD and is sponsored financially through an agreement between the Institutt for Energiteknikk (IFE) of Norway and a number of participating organisations throughout the world.

Conditions in the Halden reactor are particularly well suited to studies of fuel performance. The boiling conditions ensure a constant coolant temperature, and hence a well defined boundary condition from which to assess thermal performance from measurements of centreline fuel temperatures. Also, the low system pressure of 32 bar and low fast flux ensures negligible clad creep down, thus removing one parameter from through life assessments of fuel dimensions and temperature. However, when more prototypic conditions are required, dedicated in-pile loops are available to simulate the thermal hydraulic conditions of temperature and pressure as well as neutron flux spectrum for PWR, BWR and most recently, Advanced Gas Cooled Reactors (CAGR) as operated in the U.K.

This report outlines some of the experiments that have been performed in the Halden reactor and the most important data that they have provided which are available for use in fuel performance studies. As to be expected in a Project that has many years of experience and data production, several reviews of individual topics have already been written. This present report has made extensive use of these with the aim of demonstrating the extent of the information available collated in a form that is most useful to code developers.

The Experimental Programme

The Halden experimental programme is conducted in two ways. The first is an agreed programme of work over three year periods. This is called the Joint Programme, and all the data generated are available to the Halden Project sponsors for their own use. Although the results are proprietary, there has been a general rule that information is disclosed after a period of five years. The second is a series of bi-lateral experiments performed by Halden staff specifically for member organisations. These are funded entirely by the sponsor and the data are only disclosed to other Project members at the sponsors discretion. When discussing the data available from The Project, the degree of access will be indicated. Although this report is concerned only with fuel and materials irradiated in the HBWR, it should be mentioned that The Project also carries out extensive Man

Machine Interaction studies on the same Joint Programme and bi-lateral bases for both the nuclear and non-nuclear industry.

Each Halden reactor experiment is identified by an *I*nstrumented *F*uel *A*ssembly number (IFA). This refers to the rig design which can be re-used for a number of experiments by reloading with a succession of different fuel rods. Thus the unique experiment identifier also includes a loading number. IFA-562.2 for example refers to an assembly, IFA-562 which was first loaded as IFA-562.1 to investigate the effect of pellet surface roughness on thermal performance, but was subsequently reloaded with a completely different design of fuel rod to investigate the thermal response and fission gas release at very high burnup.

The experiments performed either address single effects e.g., fuel temperatures, fission gas release, dimensional changes, waterside corrosion etc., or, because of extensive in-pile instrumentation, the combination of centreline thermocouples, pressure gauges and extensometers, integral behaviour is also available. These experiments are particularly useful for code validation because they test simultaneously code predictions of several parameters.

Each experiment is contained within a Zircaloy shroud thus isolating the assembly coolant and thermal hydraulics from the reactor pool. Within the shroud there are: inlet and outlet turbines for flow monitoring and inlet and outlet coolant thermocouples. These are used in conjunction with miniature neutron detectors to accurately define the axial and radial power distribution of the fuel in the assembly.

Fuel centreline temperatures are monitored using W3%Re/W25%Re thermocouples, although other thermocouples are also employed depending on the temperature range to be measured. More recently an expansion thermometer design has been developed. The advantage of this method is that unlike thermocoupled rods with permanently installed cabling, these can be loaded and unloaded at will. Differential transformers are extensively used in reactor for a number of applications to measure: rod pressure, fuel and clad elongation and clad diameters. The use of He-3 coils or movable absorber shields has made possible the power ramping of individual assemblies without changing appreciably the integrated power of the reactor nor affecting the steady state operation of other experiments irradiated concurrently. The periodic use of these features has enabled studies of power cycling and load following regimes.

The in-pile instrumentation is continuously logged by a dedicated computer at 15 min intervals throughout the whole of the reactor operating periods. Faster logging speeds can be instigated for individual assemblies if special experiments are being performed. Also, in the event of a reactor scram, the logging speed of pre-defined experiments is automatically increased to obtain kinetic data. The range of experiments and their instrumentation to be included in this summary are given in Table 1, taken from HWR-302, Reference [1].

In the main, the experiments have used fuel rods which, apart from their length which seldom exceeds 1 m and more usually 500 mm or less, conform to typical BWR and PWR design. The usual materials used are sintered UO_2 pellets clad in Zr-2 unless otherwise stated. Material and design variables studied extensively include: fuel density and grain size, hollow and solid pellets, fuel-to-clad gap dimension, fill gas composition and pressure. Other studies have included comparisons with sphere-pac, MOX and doped fuel as well as cladding with different compositions. In addition to the development of dedicated loops, a further important development has been that of re-instrumentation of fuel and cladding pre-irradiated outside of the Halden reactor. This has meant that high burnup studies have been undertaken without having to wait for extended burnup accumulation.

More recently there has been the introduction of non-prototypic experiments designed to provide specific materials properties data. In this category are pressurised tubes to provide information on clad creep rates, and the isothermal irradiation of UO_2 disks to provide information on fission gas diffusivity and thermal conductivity as a function of burnup.

CHAPTER 3

DATA REQUIREMENTS

Data can be divided into a number of categories depending on the application. In this respect, the data are not of universal interest. The simplest division is into the three broad categories:

- *Data useful for model development and validation***,** e.g.: radial flux depression, fuel creep, fuel densification and swelling and clad creep down. These are the 'unsung needs' of the code developer, not often apparent in code predictions but essential to obtain a good description if reliable predictions are to be obtained. Very often these data require special measuring techniques and non-prototypic rig designs.

- *Data of direct relevance to licensing requirements*, e.g.: fuel temperatures, stored heat, fission product release and rod internal pressure, waterside corrosion. Such data are of particular use for validation purposes.

- *Data for fuel development and optimisation*, e.g.: performance of fuel variants and new cladding materials, effect of changes in fuel design. These data are of most interest to fuel vendors in developing and supporting new products.

Although the groupings above are interesting, and they do help focus on why the data are needed and the use to which they will be applied, the grouping is not of much help in structuring the presentation of this report. In which case, a more phenomenological approach will be adopted, with the data available presented under the following headings:

- Radial Flux Depression,
- Thermal Performance,
- Fuel Densification and Swelling,
- UO_2 Grain Growth,
- Fission Product Release,
- Clad Properties,
- PCMI - Pellet Clad Mechanical Interaction,
- Integral Behaviour,
- High Burnup Effects.

CHAPTER 4

EXPERIMENTS AND DATA AVAILABLE

4.1 Radial Flux Depression

Before considering thermal performance and the fuel and gap conductivities, it is worth considering what data are available on radial flux depression. RFD occurs because of the self shielding of fissile nuclei such that the power production at the centre of a fuel rod is slightly less than that at the surface. This is an important factor as it influences the radial temperature distribution across the fuel, the local inventory of fission products and hence their release. RFD is influenced by a number of factors including: fuel enrichment, pellet diameter and neutron flux spectrum. In Halden, the enrichments are rather higher than commercial LWRs, 7 to 10 % compared to 3 to 5 % and the spectrum is softer.

Data are available from PIE of a small number of Halden irradiations as given in the table below, (HWR-75, [2]). Most codes today use one of two treatments to calculate radial power distribution, the first is a simple Bessel function series which is a good fit to low burnup data, or the RADAR model, [3], which is more accurate at high burnups. However, with the interest in high burnup performance and the build-up of plutonium in regions near the pellet rim, new models are being developed, for example, TUBRNP at the TransUranium Institute, Karlsruhe, [4].

Fuel	Type of Measurement
Two sections from rod 5 of IFA-180 irradiated for two months to 1.37 MWd/kgUO_2	Transverse gamma scanning for the radial distribution of ^{95}Zr, ^{95}Nb and ^{134}Cs. This last was very weak as to be expected from the low burnup.
UO_2 pellets from the peak burnup position of IFA-431 at 4.8MWd/kgUO_2	0.5 mm cores removed across two diameters; samples taken from near the rim, mid and centre pellet positions. Measurements were taken of the radial burnup radial plutonium distribution
IFA-411 at 29.5 MWd/kgUO_2	Relative concentrations of Zr/Nb across diameters using transverse gamma scanning.
IFA-211 at 23 MWd/kgUO_2	As above, also relative concentrations of ^{235}U and ^{239}Pu.

4.2 Thermal Performance

Thermal performance occupies the most important aspect of fuel performance assessment. Not only is it extremely important from a safety point of view, particularly in the avoidance of fuel melting and loss of geometry, but many of the material properties of interest e.g., transport properties like fuel creep and fission gas release are exponentially dependent on temperature. Thus, in order to provide reliable assessment of fuel performance it is critical to calculate temperatures and their distribution as accurately as possible. For this reason, the Halden programme has devoted a considerable amount of attention to obtaining thermal performance data, and this is considered in some detail below.

It is assumed that the thermal hydraulic heat transfer on the outer surface of the cladding are known and obey standard equations. The main thermal resistance in the fuel rod is that of the fuel to clad gap and the thermal conductivity of the pellet. Any oxide formed on the outside of the clad will also contribute, and this effect becomes important at high burnup. The conductivity of zirconium oxide will be considered later in section 4.5.

In the next two subsections, data will be summarised from in-pile thermocouple measurements at the beginning-of-life and through the subsequent irradiation. Unfortunately it is very difficult to separate the contributions of the gap and fuel conductance to the overall behaviour, although some degree of separation can be made through the time dependence of the temperature evolution. The factors that influence these two phenomena are given below:

Gap Conductance	Fuel-to-clad gap separation surface roughness of fuel and cladding fill gas composition (helium, argon, xenon) fill gas pressure
Fuel Conductivity	Density cracking composition, additives, MOX, Gd etc. irradiation

4.2.1 Beginning-of-Life Behaviour

At the start of an irradiation, there is less uncertainty about material properties and dimensions than at any other time, and the start-up ramp and any subsequent power ramp taking place shortly after start-up provide a wealth of information, on gap conductance in particular.

In order to develop or validate a gap conductance model it is necessary to ensure the calculation reproduces the effect of gap and fill gas composition as faithfully as possible. To do this, experiments using high density fuel are preferred. In this way, changes in gap dimension due to densification are kept to a minimum. The data available on standard fuel pellets with densities ≥ 95% TD are given in the following Tables 2(a) to 2(f):

Helium fill gas

Small gap rods, <100 µm	Table 2(a)
Intermediate gap rods, 100 ≤ gap <200 µm	Table 2(b)
Large gap rods, ≥ 200 µm	Table 2(c)

Xenon or mixed composition fill gas

Small gap rods, <100 µm	Table 2(d)
Intermediate gap rods, 100 ≤ gap <200 µm	Table 2(e)
Large gap rods, ≥ 200 µm	Table 2(f)

Of particular interest are the data from the gas flow rig, IFA-504. This assembly contained 4 rods equipped with thermocouples at both ends of each rod. Very early in life opportunity was taken to measure temperature versus power in a succession of ramps to normal operation, with different gas compositions, helium, argon and xenon. Thus for the same rods and hence identical fuel structure, unique data are available on the effect of fill gas composition, see Figure 1.

The effect of gap size on conductance is ably demonstrated for the three helium filled rods in the assembly IFA-509, see Figure 2.

The effect of surface roughness on gap conductance was investigated in IFA-562.1 where two manufactures each supplied fuel of two different surface finishes. Despite pre-conceived views of its importance, the experiment showed little effect of roughness on the performance, [5].

Examination of the data shows that under identical conditions, there is an intrinsic scatter in thermal performance. This is partly due to the stochastic nature of the process, in particular, the different amounts of fuel cracking, fragment relocation fuel and the effect on the gap size. Also there would appear to be a dependence on manufacturer and the route they use for fuel production.

Immediately after start-up, the fuel commences to sinter, the extent depends principally on initial density, but also the pore structure. Pores ≤ 1 µm sintering faster than larger pores and in some instances when 'pore former' has been used during manufacture, very little densification takes place at all. Thus once the initial data have been used to establish a gap conductance model, it is possible to use subsequent early life behaviour, both temperature versus power in ramps or temperature at constant power to determine the densification kinetics from changes in gap size. This is best studied using xenon filled rods because of the dominance of gap conductance to the overall thermal behaviour due to the poor thermal conductivity of the gas. Such variations in behaviour demonstrating densification are shown in Figure 3. Further evidence of densification will be considered from fuel stack length changes in section 4.2.

Data for low density fuel, < 95 % TD, fuel variants like sphere-pac, MOX and doped fuel are given in Table 2(g).

4.2.2 Through-Life Behaviour

Although all experiments operate at a variety of power levels throughout their life depending on reactor conditions, it is possible to separate out temperature data through life within a constant small band of power. This is very instructive as the evolution of fuel structure can be discerned from the behaviour.

Figure 3(a) is one such example from the xenon filled rod 1 of IFA-562.1, where centreline temperature is plotted against burnup for the two power levels 20 and 30 kW/m. It can be seen that initially the temperature increases as the gap opens due to fuel densification. Just before reaching 2 MWd/kgUO_2 the temperature starts to fall as densification ceases and the gap progressively closes due to solid fission product swelling.

This is typical behaviour of a xenon filled rod, or at least for a rod whose thermal performance is dominated by gap conductance. Figure 3(b) shows the equivalent plot for the helium filled rod 11 in the same assembly. There is an initial increase in temperature as before, but this time, after densification is complete, the temperature continues to rise monotonically. In this case the thermal performance is dominated by the fuel conductivity which is progressively degraded with increasing burnup.

An extremely good example of these effects demonstrating the competition between gap closure and degrading fuel conductivity is shown by the four rods in the gas flow rig IFA-504. Although the rods are filled with helium for most of their irradiation, periodically the gas has been exchanged for argon. Thus for the each rod, temperature data are available for the two different fill gas composition as shown in Figure 4. The figure shows temperatures falling with burnup when the rods are filled with argon, yet for the same rod, the temperature rises with burnup when filled with helium. For a good representation of the thermal performance of fuel rods it is very important that code calculations reproduce this behaviour.

To define the degradation of conductivity with burnup it is preferable to use data from small gap helium filled rods which have operated at powers sufficiently low as to preclude poisoning of the gap with released fission gases. A list of experiments which have been used for such an analysis is given in HWR-299, [6], and reproduced here in Table 3.

Any rod operating at a high enough power and fuel temperature will eventually release fission gas into the fuel- clad interspace. Although this does not affect the gap conductance for xenon filled rods, the gap conductance of helium filled rods is considerably reduced, and can result in a significant increase in fuel temperatures. The assembly IFA-432 contained helium filled rods 1, 2 and 3 with gaps of 230, 380 and 70 µm respectively and was operated in such a way that the gap in both large gap rods became contaminated whereas the lower temperature small gap rods remained free of fission gas. The relative behaviour of these three rods can be see in Figure 5 taken from HWR-215, [7], where the increase in temperatures in rods 1 and 2 above 4 MWd/kgUO_2 is due to the released fission gas.

Further examples of this behaviour are given in the table below. The timing of fission gas release can be very difficult to predict accurately, and comparison with these type of data is a severe test of a codes predictive capabilities.

IFA-No.	Comments
410	Rods 1 & 2 (400µm gap) when peak positions crossed the empirical FGR threshold at ~2MWd/kgUO_2; compare to Rod 3 (µm gap) which did not cross until 8 MWd/kgUO_2
411	Thermal feedback noted on peak position crossing empirical FGR criterion at ~2MWd/kgUO_2
432	Rods 1 & 2 when peak position crossed FGR criterion at ~4 & ~2 MWd/kgUO_2 respectively. Compare to small gap rod 3 which did not show feedback effects.
505	Rod 924D (TF-4) on crossing empirical threshold at ~25-27 MWd/kgUO_2.
513	Distinct increase in temperature response at constant power for rods 2 & 4 immediately after ramp at ~14 & 15.5 MWd/kgUO_2 respectively.

In order to predict fuel behaviour in over power transients, especially rapid transient as in RCCA ejection faults, it is necessary for a code to have the capability of calculating the fuel temperature response to power changes. When the power is suddenly increased, the temperatures lag behind the steady state values because of the thermal inertia of the fuel. Data are very sparse and are confined to experiments performed in three assemblies. Information on these experiments can be found in HPR-242 for IFA-429, [8], HPR-229 vol. II paper 9 for IFA-507, [9] and HPR-235, [10] and 242 for IFA-509, [8].

On the other hand, the lag in fuel temperature on power decreases as in reactor scrams is also important as it dictates the rate of release of heat to the coolant which is important in describing the sequence of events in some coolant accidents, large break LOCAs for example. As mentioned previously, the instrumentation of the Halden reactor has been arranged to increase the logging speed of certain IFAs in order to obtain data on their response during any intentional or unintentional scram. The earliest report on scram analysis is given in HPR-276, [11], including a description of the Halden SCTEMP code. This report demonstrated that , not surprisingly, the time constant increased with gap size, and was larger for xenon filled rods than for helium filled rods. Further work was reported in HWR-249, [12] which concluded that the time constant was increased in rods after fission gas release and even in low powered helium filled rods without fission gas release there was a slow increase in time constant as the fuel conductivity degraded with increasing burnup. Illustration of these effects are given in Figure 6.

Evaluation of the heat that is released in a reactor scram relies on the correct representation of the radial temperature profile across the fuel rod, since it is the integrated temperature that controls the amount of heat stored. Recently Halden have performed experiments to measure directly the heat released in a scram, and data on this can be found in HWR-300, [13].

4.3 Fuel Densification and Swelling

In the previous section the influence of fuel densification and swelling was mentioned in respect to the influence they had on the evolution of the gap with irradiation. A more direct method of measuring these phenomena is through fuel stack elongation. Several experiments have been performed where the length of the fuel stack has been measured using the movement of an iron core attached to the fuel within the coils of a transformer attached to the assembly structure. These instruments usually referred to as ‘EFs’ have worked satisfactorily over many years irradiation and data are available up to very high burnup; details of two examples follow.

IFA-409.2 contained 6 short low enriched rods with 230 µm gaps filled with helium at atmospheric pressure. Irradiation conditions were such that fission gas release and swelling was prevented and the resulting axial length changes were due only to densification and solid fission product swelling. The experiment compared the performance of fuel of different density and grain size:

Rod no:	8D1	8D2	8D3	8D4	8D5	8D6
Density %TD	92.7	92.5	94	92.6	96.1	99.0
Grain size, µm	?	3.7	62.5	5.1	69.5	62.5

Throughout the experiment, the rods were transferred to IFA-408.2 and IFA-515.4, further details can be found in HWR-200, [14]. Data are available in excess of 30 MWd/kgUO_2 as:

ΔL/L versus power at 0 and 30 MWd/kgUO_2
ΔL/L versus burnup at hot stand-by

The densification behaviour extended to between 2 and 8 MWd/kgUO_2 and depended on the initial fuel density; after this burnup the rods showed a uniform rate of growth of 0.77 to 1.03% ΔL/L per 10 MWd/kgU, see Figure 7.

IFA-401.2 contained 12 short high enriched rods with 350 µm gaps filled with helium at atmospheric pressure. Details of 3 rods can be found in HWR-252, [15]:

Rod no:	201	202	203
Density %TD	94.5	91.5	91.9
Grain size in µm	25.26	25.27	6 - 8

Data are available as above in excess of 54 MWd/kgUO_2.

4.4 UO_2 Grain Growth during irradiation

The Halden database of grain growth measurements consists of over 170 fuel sections taken from 30 assemblies. This database has been reviewed in HWR-164, [16] and a small number of cases compared with grain growth models. The selection process was very rigorous, rejecting: early data where the irradiation history was uncertain, experiments where no thermocouples were available for temperature measurement and cases where no growth was observed. The cases which were retained are given below.

IFA-No.	Burnup MWd/kgUO_2	Temperature history ^oC	Comment
223	20	1600 falling to 1200	-
224	9	1700-1800	Substantial grain growth and columnar grains formed.
410	14	1000-1100 with peaks to 1400	Very little growth observed.
411	25	1200-1400 1200-1500 1400-1600	Three separate sections.
505	12 5	1600 1700	Two sections.
522.1	9	1200 plus short period at 1400, 1900 at end-of-life	Two sections one showing columnar grains. Good data to test grain boundary pinning models

More recent data are now available not covered in this review, in particular, from IFA-562.1 where the assembly was intentionally ramped at the end of the irradiation in order to promote grain growth.

4.5 Fission Product Release

4.5.1 Radioactive Fission Products

The natural consequence of the fission process is the splitting of the fissile nucleus into two fragments which eventually become new atoms with appropriate chemical behaviour. The maxima in the doublet distribution of mass numbers occur in the regions 90-100 and 140, thus giving high yields to the rare gas species krypton and xenon and the volatile species iodine and caesium. Concerns arise when these species are released from the fuel matrix because they challenge the clad integrity both through increased internal pressure and also Stress Corrosion Cracking (SCC) and the concomitant escape of radioactive iodine and caesium, (among others), represent a radiological hazard to reactor operators and the general public.

There have been many studies of the operating regime and materials properties in order to reduce the release of these species and maintain safe reactor operation. Although it is the radioactive isotopes of the volatile species which are the major hazard, only their gaseous precursors or stable rare gases can be readily measured in-pile.

The fractional release of radioactive krypton and xenon of half lives between the 5 day ^{133}Xe and 32.3 sec ^{90}Kr have been measured under various conditions in the prototypic gas flow assemblies: IFA-430 (2 rods), IFA-504 (4 rods) and IFA-558 (6 rods). More recently release measurements have been made from rodlets containing UO_2 disks irradiated under isothermal conditions in IFA-563. In all cases the fractional release defined as:

$$(R/B) = (\text{Release Rate from the fuel})/(\text{Production rate in the fuel})$$

conforms to the general equation for (R/B) < 10 %:

$$(R/B) = (S/V)\,(\alpha D/\lambda)^{1/2} + (R/B)_{\lambda\text{independent}},$$

where D is the diffusion coefficient, a is a constant to account for diffusion as precursors and λ is the radioactive decay constant. An example of measurements illustrating this behaviour is given in Figure 8. These data are reported in several Halden reports issued during the life time of the experiments. (HPR-326, [17], HWR-231, [18] and HWR-332, [19]). Data from IFA-558 are noteworthy as measurements were taken of both radioactive and stable fission gas release; such a combination represents very valuable and unique data, HWR-258, [20].

4.5.2 Stable Fission Gas Release

Although it would be ideal to split the fission gas release (FGR) database into: release under steady irradiation conditions, release during single over power transients, release during multiple transients and cycling conditions, the practicalities of operating a test reactor are that such a division is not easily attained. Identification of intentionally ramped and power cycled fuel is straight forward and will be treated as separate categories, but it is very unusual to have fuel that has experienced ideal steady and constant irradiation conditions. Invariably fuel operated under constant conditions experience changes in power as a result of loading and unloading of adjacent assemblies or the need

to move the assembly in order to prevent the assembly power decreasing too much due to burn-out of the fissile uranium isotope. In which case, what was planned as constant irradiation conditions becomes a varied power history with a series of inadvertent power transients of various magnitudes and duration. The alternative scheme of division, adopted here, is to split the database on nominally steady irradiation conditions into cases where the final fractional release is within defined limits.

A common and now well established feature of fission gas release observations is a threshold for conditions, below which the fractional release remains low typically less than 1 % and often very much less than this value. Above this threshold, release values rise rapidly and under extreme circumstances exceeds 10 % in conditions only to be experienced during overpower transients or accidents. Halden has made an extensive study of fission gas release using rods equipped with pressure gauges. Their observations have been embodied in an empirical criterion for this threshold in terms of centre fuel temperature (TF) versus burnup above which release in excess of 1 % is to be expected, [21]:

$$\text{Burnup}(\text{MWd/kgUO}_2) = 0.005 \exp(9800/\text{TF}(^{o}\text{C}))$$

This correlation was devised using a data base of 36 fuel rods operating in Halden under different conditions to burnup levels of 38 MWd/kgUO_2 rod average and 44 MWd/kgUO_2 peak. The database is now more extensive comprising some 70 cases:

FGR < 1%	13 cases
1 < FGR < 10%	23 cases
10% < FGR	34 cases

The most difficult cases for modelling are in the vicinity of 1% release, where it is critical to have a correct prediction for the onset of grain boundary interlinkage. In the interval 0.8 to 5% release the Halden database contains 13 cases which provide good data for model development or a challenge for existing model validation.

Data on release during rapid overpower transients were obtained in the IFA-429 series of experiments, [22, 23], where the assembly was fitted with an absorber shield which could be rapidly lifted to expose the fuel to a series of rapid transients. The assembly has provided excellent data on the kinetics of release during multiple short transients of short duration and the values of rod burnup and release are given in Table 4(a).

Since perfecting a method of re-instrumenting pre-irradiated fuel rods, a number of experiments have been carried out to yield gas release data at high burnup. The re-instrumentation technique has been described in HWR-70 and requires the connection of a pressure detector to the free volume of the pre-irradiated fuel rod without the escape of the original fill gas or released fission products. At the same time, the rod is fitted with a cladding extensometer. The rod is then loaded into the assembly IFA-535 for slow power ramping effected through changes in reactor power, [24]. Fission gas release measurements and rod burnup are given in Table 4(b). Notable results from this series is a comparison of release in pressurised (32 bar) and unpressurised rods (2 bar), where the same levels of release were found independent of pressurisation. Also, in IFA-535.5 and .6, pressure measurements during ramping identified the power to initiate release as 32 kW/m in one and 35 kW/m in another two rods at a burnup of 44 MWd/kgUO_2, [25, 26].

Although it is difficult to present a concise overview, there is a wealth of information available from these experiments in the form of comparisons between rods of different design. Table 5 provides more details for some of these experiments with an emphasis on the special feature each experiment addressed.

To summarise this section, the Halden database on fission product release is very extensive and varied. It encompasses in-pile and PIE measurements of stable fission gas release as well as in-pile measurements of radioactive fission gas release. Data are available on standard and modified fuels in steady state, transient and power cycling conditions. Kinetic information is available from rods equipped with pressure gauges, and in some cases there are simultaneous measurements for fuel centreline temperatures.

4.6 Clad properties

4.6.1 Irradiation Growth

Irradiation growth of zirconium occurs differently in different directions of the zirconium lattice because of its hexagonal anisotropy . Whereas expansion occurs along the a-axis, contraction has been measured along the c-axis. In fuel rods, the grains are preferentially oriented with the c-axis in the radial direction because of the texture induced by the method of manufacture, as a consequence, irradiation growth results in an axial elongation because of the dominant expansion along the a-axis. The rate of length change of Zircaloy cladding decreases with exposure and can be described as a function of fluence by an equation of the form:

$$\Delta L/L = \text{Const} . (\Phi t)^n,$$

where $\Delta L/L$ is the growth strain, Φ is the fast neutron flux and t is time. The index n ranges between 0.4 to 0.6. Temperature effects on growth are considered to be small. Cold work adds a component of length increase in the direction of working. For cold worked Zircaloy-2, the index n may range from 0.5 to 0.9.

In the Halden reactor, the fast flux is rather low and as a consequence permanent length changes are more likely to be due to PCMI than irradiation growth. However, where irradiation growth can be distinguished from other effects, the data from Halden is in agreement with other studies, although the burnup range covered is limited, HPR-246, [38], HPR-221.07, [39].

4.6.2. Creep

The time dependent deformation of materials is enhanced by high temperatures and in a hard neutron flux. Two regimes are important with respect to the behaviour of reactor fuel rods, the first is steady state irradiation creep causing closure of the manufactured fuel-to-clad gap under the influence of the hydrostatic system pressure, the other is the transient response of the cladding to mechanical interaction with the underlying pellet (PCMI). This latter is addressed in section 4.5, but there are data available on both aspects of Zircaloy creep from dedicated Halden experiments.

IFA-414 was a high pressure rig furnished with two sets of diameter gauges 90^o apart to measure creepdown and ovalization behaviour under PWR conditions on single fuel rods. There were several loadings of this rig and the effect of cladding compressive stress was examined by using different rods filled at different pressures 1 to 27 bar. Figure 9 taken from HWR-270, [40] shows the results of one of the experiments for a Zr-4 clad rods filled with 27 bar helium.

Creepdown data were also obtained from rods base irradiated in the BWR IFA-523 and PWR IFA-524 rigs at relatively low burnups through interim profilometry measurements in the handling compartment adjacent to the reactor.

A more recent experiment, IFA-585 currently operating in the reactor is investigating creep behaviour of Zr-2 under BWR conditions and Zr-4 under PWR conditions in a rig equipped with 'booster rods' in order to enhance and harden the neutron flux. Steady state behaviour is observed using pre-pressurised segments whilst the transient response to changing stress levels is controlled by internally pressurising segments from a gas circuit. In all cases, the observations are made using diameter gauges traversing the experimental segments with in-built standard diameters as reference points.

4.6.3 Stress Corrosion Cracking

Two experiments have been conducted to investigate the effect of fission products on clad failure by Stress Corrosion Cracking. In response to questions raised by modellers, the experiments were aimed at investigating the effect of the quantity of fission products available at the time of crack initiation and propagation, and also the effect of fission product age.

The topic had been addressed by experiments in IFA 516 and the results reported in HWR-191, [41]. In this experiment, 6 rods were irradiated to a burnup of ~14 MWd/kgUO_2 before ramping to promote fission product release. The high power of 45 kW/m was sustained for 5 hrs before being reduced to 27 kW/m. Immediately on reaching this power, two rods, now containing freshly released fission products, were pressure tested and failed after a short time at maximum pressure. Two further rods were kept at low power for 10 days before being subjected to identical pressure ramps where both failed after 1 hr at the highest pressure. Inspection and PIE revealed SCC defect in only one of the rods tested with 'fresh' fission products and one of the rods containing fission products aged for 10 days.

A second experiment was designed, IFA-567 where six rods which could be pressurised from an external gas circuit were irradiated to burnups between 15 and 18 MWd/kgUO_2 before being tested individually with a pre-defined pressure ramp. The gas used prior to and during testing was chosen so that the fuel temperatures could be controlled via the gap conductance thus controlling the timing (and hence the age) and quantity of fission products present in the fuel-clad gap at the time of maximum clad hoop stress. Out of a total of 10 successful tests, two rods failed by SCC and at the time of writing, one had been subjected to detailed destructive PIE, HWR-384, [42].

4.6.4 Waterside Corrosion

Waterside corrosion of Zircaloy cladding is a potentially life limiting factor for the improvement of fuel efficiency in PWR systems since extending the residence time and/or increasing the coolant temperature increases corrosion. In a 'hot PWR plant' for instance, nucleate boiling will occur and this may lead to an increase in corrosion rate due to changes in heat transfer conditions. Load following is another operational condition which may adversely affect corrosion due to changes in local water chemistry or microstructure of the oxide formed.

IFA-560 was commissioned as a PWR rig capable of subjecting two bundles of PWR rods to coolant conditions chosen to study corrosion under a variety of well controlled conditions. Commissioning trials were performed in IFA-560.1, and the first experiment using pre-irradiated rods took place in IFA 560.2. The rods were KWU manufactured Zr-4 clad MOX fuel irradiated for 3 cycles in the KWO power plant to an average of 32 MWd/kgMOX. The fuel was mounted in two 'strings' comprising two short rodlets one above the other connected by a rod of Zr-4. The lower rodlets of each string were surrounded by a neutron absorbing shield thus depressing the power. The thermal hydraulic conditions were such that nucleate boiling occurred in the upper part of the rig whilst non boiling conditions were maintained within the shield. One string could be moved axially to simulated power cycling, and during the course of the experiment experienced 60 cycles. Oxide thickness was

measured before and after irradiation using a high frequency eddy current probe in the handling compartment located in the reactor hall. The concentration of lithium in the coolant was controlled to be within the range 1.2 to 2.3 ppm. During the course of the experiment the oxide thickness on the upper rodlet of the stationary string increased by about 12 µm whilst that on the movable string increased by about 6 µm, (HWR-236, [43]).

A second experiment designated IFA-568 commenced in June 1989, based on the previous design. The objective was to investigate the effect of increased lithium concentration, 4-4.5 ppm plus 1000 ppm boron on the corrosion in nucleate and non boiling conditions. The fuel used was 4 KWU fuel rods irradiated to an average 32 MWd/kgUO_2 during two cycles of the Gösgen reactor in Switzerland. Measurements of oxide thickness were made at the start of the experiment and periodically up to around 400 full power days of operation, HWR-333, [44].

One of the parameters of interest associated with the waterside oxide is its thermal conductivity. For modelling purposes this is required in order to calculate the temperature of the metal-oxide interface in order to model the oxidation process. Also, the extra thermal barrier is likely to increase fuel temperatures and hence rod internal pressure at high exposure. It is important that measurements of conductivity are made in-situ, thus including any effects due to the presence of the coolant. For this reason an experiment has been initiated in Halden to compare the axial expansion of two rods operating under identical conditions, one with oxide, the other without. These data are very recent and restricted to Halden Project participants only.

4.7 Pellet-Clad Mechanical Interaction

Since the commissioning and operation of their first rig in 1969 to study pellet-clad mechanical interaction effects, IFA 118, the Halden Project have constructed some 13 assemblies to study various aspects of the phenomenon. The instrumentation used on these rigs comprises: fuel and cladding extensometers and diameter gauges. The extensometers provide information on the absolute and relative axial strain of the fuel and cladding, whilst the diameter gauges provide data on diametral strain and clad ridging. The ultimate use of these data is to develop an understanding and models predicting clad strain due principally to dimensional changes in the underlying fuel and to be able to predict situations where clad integrity may be prejudiced. With such a large number of assemblies, there is clearly a vast amount of data on the topic and an excellent review of the database was written by Halden staff in 1983, (HWR-89, [45]). The assemblies covered by this review and the instrumentation they have is given in Figure 10 taken from the report.

It is anticipated that from a fuel modelling point of view in order to develop or validate models, the first interest would be in data on axial elongation with the focus on predicting the onset of PCMI and the factors that influence it. Once interaction has taken place, the next most important information is the amount of strain induced in the clad by the fuel, that is, the average diametral strain. Additional to this is the strain enhancement at pellet ends caused by wheatsheafing of the underlying pellet. This is where the maximum clad strain takes place and is the most probable site for crack initiation and eventual failure. The review of data presented here will adhere to this order: axial elongation and onset of PCMI, data on average diametral strain and finally data on ridging.

4.7.1 Axial Elongation

In an ideal wide gap rod, the cladding extends longitudinally during a power ramp solely by thermal expansion until the pellet-clad interface is closed and the cladding extension is driven by the expansion of the fuel stack. In this idealised situation, the point of axial interaction is sharply defined, but in practice this is not the case. Although the point of interaction is clearly evident, the behaviour of the cladding is that of a smooth transition between the two regimes. Experiments involving rods fitted

with elongation transducers, e.g., IFA-118, IFA-215, IFA-507 and IFA-509.1 have confirmed expectations that the power for the onset of axial interaction increases with increasing gap size but decreases with burnup as the gap is closed by fuel swelling; see for example the data presented in Figure 11.

The following is a summary of observations on axial elongation, the parameters affecting its magnitude and the experiments in which the observations were made. Because of the diversity of measurements and observations, this section is extensively referenced back to the original Halden reports.

The degree of axial elongation after PCMI is characterised by the generalisations listed below:

- It is little affected by clad thickness in the range 0.40 to 0.75 mm, as found in IFA-118, [46] and IFA-215, [47];
- It increases slightly with increasing pellet length. This was most pronounced in the early IFA-118 but was found to be less pronounced in IFA-411, [48];
- It depends on the geometry of the pellet end. It decreases in the order: flat ended, dished, chamfered, as demonstrated in IFA-118, but the effect was less pronounced in IFA-410, [48]. Also, the effect appears to reduce with burnup;
- It is less in rods containing vipac and annular pellets, IFA-509.2, [49], IFA-227, [45]. There appears to be little effect of lubricated pellet-clad interface than for standard solid pellet fuel, IFA-413, [48];
- There is a dependence on fuel density; interaction is generally greater in high density fuel. However, there is little difference between high density and *stable* low density fuel, e.g., IFA-404.2, [48, 50] and IFA-402, [51] where 95% and 85% dense fuel was compared;
- The behaviour of MOX fuel does not differ significantly from standard UO_2, IFA-118;
- Interaction is greater in long than in short rods, see Hazel et al. Reference [52].

When held at high power, there is a pronounced relaxation in the axial clad strain which can continue over many days, e.g., IFA-507, [53, 54]. The rate of relaxation is not affected appreciably by power cycling, IFA-519.8 and IFA-550.2, [55]. Relaxation is greatest in low density unstable fuel, IFA-404.2, [48, 50].

Clad elongation during ramping followed by constant power, is comparable with ramping and cycling, for PWR and BWR conditions in the IFA-520 and IFA-525 series of experiments, [35].

4.7.2 Diametral Strain

Diametral strain, both elastic and plastic, during and after power ramps has been extensively studied using in-pile diameter gauges that can traverse the length of a fuel rod in one or more orientation. The effect of gap size and ramping at different levels of burnup can be found in the results from IFA-420.3, [45] as well as IFA-508, [56] and IFA-509.1, [57], where the evolution of diameter with burnup approaching 30 MWd/kgUO_2 was followed along with clad elongation and fuel stack length.

In an open gap rod, at the onset of PCMI, experiments in IFA-227 and IFA-508 showed that the build up of axial stresses in the cladding caused lateral contraction which reduced the clad diameter, particularly at mid pellet positions, and thus lowered the power for fuel to clad contact.

Factors which have been found to affect diametral strain are given below:

- There is a smaller effect of fuel density than for axial deformation. Again, diameter increases in power ramps are greatest in high density fuel rods but are little different than for low density fuel that is stable against sintering. Data on this was obtained in IFA-227, [45] and IFA-404.2, [48, 50];

- For the same power conditions, the diametral expansion of hollow pellet fuel is less than for solid pellets and the amount of relaxation is greater. Examples of this comparison are presented in Figure 12 taken from IFA-509.2, [49]. This also applies to power cycling where hollow pellet fuel experiences less damage than for solid pellets;

- Greater permanent strain is induced in fuel subjected to rapid power ramps compared to slow ramps where the strain can be purely elastic and recoverable; IFA-436.1 and .2, [58].

4.7.3 Ridge Formation

Diameter gauge measurements have revealed the presence of increased dimensions at the position of pellet ends during and after power ramps resulting from the wheatsheaf or hourglass shape adopted by the underlying pellets. The is on account of the poor conductivity of the fuel and the consequent differential thermal expansion caused by the temperature difference between the interior and exterior of the pellets. A good example of the diameter change during a power ramp at pellet ends and mid pellet position is given in Figure 13 from IFA-414.5, [59]. Ridge formation to a greater or lesser extent is found in all small gap rods when power ramped, e.g., IFA-227, IFA-404, IFA-512.7, [60], and IFA-436.1 and .2, [58] as well as in the BWR and PWR power ramping loops IFA-520 and IFA-525 respectively, [35].

The experiments support the general observations below:

- Ridges only occur in small or closed gap rods and the height increases with ramp power, IFA-508, [56];

- Ridging is more pronounced in dished pellets than in flat ended pellets, IFA-227 and IFA-525, [45 and 56];

- Ridging is more pronounced in high density fuel than low density unstable fuel and vipac, IFA-227, but data from IFA-402.2, [51], first ramp qualifies the statement regarding the effect of density because of the insensitivity observed. There is clearly a link between observations in densifying fuel and the power and duration of the power ramp;

- Clad wall thickness had only a small effect on ridge height as observed in IFA-508, [57];

- During periods of sustained high power or even periods of cycling between high and low power, diameter changes can occur in either direction, shrinking at low burnup due to densification or expanding due to fission gas swelling. However, during these periods the observation is that ridge height always decreases, see for example IFA-512.7, [60], also the ramped and cycled rods in the BWR IFA-520.7 (cycled), IFA-520.8 (steady power), IFA-525.9 (cycled) and IFA-525.10 (steady power), [35].

4.8 Integral Behaviour

There are many instances where assemblies with nominally identical rods are irradiated simultaneously with different instrumentation. In some cases, individual rods contain more than one type of in-pile sensor. In both cases, the combination of measurements affords an excellent description of fuel behaviour which greatly assists model development or, alternatively, provides very exacting tests for code validation. This section describes some of the best well instrumented assemblies and the combination of measurements available.

IFA-429 *TFs and PFs*

This was a long and successful experiment, originally sponsored by the USNRC and EG and G in 1975, with PWR-type rods irradiated in three clusters under normal BWR conditions, some to burnups in excess of 50 MWd/kgUO_2. Only two rods were fitted with conventional thermocouples and one of these continued to function up to a local burnup of 50 MWd/kgUO_2. Two series of rapid ramp experiments were carried out on a limited number of rods in this rig at high burnup by lifting silver absorbing shields but the rods containing TFs were first discharged.

IFA-431 and IFA-432 *TFs, PFs and ECs*

IFA-432 and its fore-runner were two fuel assemblies with six rods in a single cluster and almost identical component rod characteristics. IFA-431 was loaded in June 1975 whilst IFA-432 was loaded in November 1975. IFA-431 generally operated at lower ratings. The xenon filled rod 4 in both assemblies included special mechanical constraints at either end of the fuel stack, such that at the lower end of each rod the pellets were held eccentrically and at the upper end concentrically. The instrumentation comprised a total of 3 pressure transducers, 6 clad elongation detectors and 12 centreline thermocouples for IFA-431 and 9 in IFA-432.

IFA-504 *TFs with different fill gases, hydraulic diameter measurements and radioactive FGR*

The assembly is still in the reactor at the time of writing and comprises four fuel rods containing different fuel variants: two standard grain size rods with fuel supplied by different manufacturers, one containing niobia doped large grain fuel and one hollow pellet rod. Each is connected to a gas flow system which can flush the rods with gases of different composition, xenon, argon or helium at pressures in the range 1 to 30 bar. Exhaust gas is counted for released fission products by a gamma spectrometer.

IFA-505 short rods, TFs and end of life FGR

IFA-505 commenced irradiation in April 1978 and was designed to produce in-pile thermocouple decalibration data as well as general fuel performance information. The experiment initially contained 24 minirods with a wide range of different characteristics. 16 of these rodlets had fuel thermocouples. The total irradiation period continued until August 1986 and consisted of five different loadings. Various rodlets were removed and replaced after each loading for the purpose of examining the thermocouple decalibration effect. They were then replaced with non-thermocoupled rods. Altogether 18 different rodlets were substituted at different stages, 9 of which were xenon filled. The rodlets experienced a final ramp to higher ratings at the end of loading cycle five.

IFA-509 *TFs, ECs, FCs and diameter gauges*

The assembly contains three rods and has been operated through many loadings to generate information on several aspects of fuel performance comparing rods of different gap size, hollow versus solid pellets, standard versus doped fuel. The combination of variants and instrumentation, sometimes different depending on loading offers unique integral effects data.

IFA-513 *TFs, ECs and PFs*

IFA-513 was loaded in October 1978 and was a complementary HP/USNCR experiment to IFA-431 and IFA-432. Of the six rods, two were manufactured with known mixtures of xenon and helium as fill gas. The rest had 100% helium. Some periods of high power operation were introduced and there was also a large power ramp at about 15 MWd/kgUO_2. Each rod had two centre thermocouples, a pressure transducer and cladding elongation sensor. The experiment was discharged in November 1989 after a total of four loadings. Some problems had been encountered with water ingress in some of the rods. Three rods lasted with integrity to a burnup of nearly 30 MWd/kgUO_2.

IFA-522 *TF, EC and gap meter*

The gap meter rig IFA-522 allows in-reactor measurements of fuel/cladding gap width, rod diameter, cladding elongation and fuel temperature, all in one single rod. A travelling gauge allowed cladding diameter profiles to be made at suitable time intervals. The fuel/clad gap was measured by a squeezing technique at selected axial locations. Altogether four different rods with the same dimensions but various enrichments have been irradiated separately in consecutive loadings. For the second loading a rod containing xenon fill gas was used, which was otherwise identical to the helium filled rod in loading 1. In all the others the rod was helium filled.

Temperature readings from the first two loadings were the most satisfactory and can be used for direct comparison of the effect of helium and xenon filling.

IFA-552 *Mix of TFs, PFs and ECs in 130 and 180 µm gap fuel*

This experiment was designed to study both thermal and mechanical behaviour and was loaded in June 1984 and achieved a burnup in excess of 30 MWd/kgUO_2 before discharge. There were 8 rods with 5 thermocouples, 5 cladding extensometers and 3 pressure transducers. The fuel of two gap sizes was irradiated at modest ratings with two prolonged periods at higher rating. All rods showed a very consistent behaviour.

IFA-562.1 *Mix of TFs and ECs in He and Xe filled rods*

The assembly consisted of 12 rods irradiated in 2 clusters containing fuel of two different manufacture. All were small gap rods, 4 rods in each cluster were filled with xenon. Each rod had a cladding elongation detector which was used to assess when hard fuel-clad contact occurred. The assembly produced useful data on the effect of pellet surface finish and the effect of fill gas composition for closed gap conditions.

4.9 High Burnup Effects

Although many of the assemblies already mentioned have provided data at high burnup, this topic is considered separately because there is a need to compare code predictions extrapolated outside the range of burnup used for their development to see whether or not modifications are required to the models and correlations used for material properties. Also, there is the possibility that new models are required to describe high burnup behaviour. One such requirement already covered is the need to formulate the degradation of fuel thermal conductivity with burnup. Up until very recently, such a phenomenon was not an integral part of fuel performance codes, however, with the extension of discharge burnup, it is now a necessity.

Recent experiments and PIE have identified what appears to be an additional gas release mechanism that becomes significant at burnup levels in excess of ~50-60 MWd/kgUO_2. This has been ascribed to the accumulation of plutonium and enhanced fissioning in the rim of the fuel pellet. Data are needed therefore to extend current gas release models to include this phenomenon either in an explicit or implicit way. Table 6 gives a list of assemblies and their burnup as of 31 December 1993. Many are still in the reactor and hence their burnup will be in excess of the figure given. It should be noted that the Halden reactor has a softer neutron spectrum than power reactors so this must be born in mind when studying high burnup data.

CHAPTER 5

FUTURE PROGRAMME

5.1 Data Available from the Halden Project

This report has reviewed the data that are available to fuel modellers from the Halden Project. The report only serves to identify the data available and not to present it in the most useful form; that is the subject of the next stage of the exercise.

It is clear that the quantity of information is very large and that some prioritisation is necessary in order to start the process of dissemination. Some of the databases are small and hence the totality of the data available must be used, in particular, grain growth, solid fission product swelling etc. In other cases, the database is too large for all the cases to be useful. With the help of Project staff, experiments have been categorised into topics and the following is a list of the experiments given the highest priority because of the quality of the data produced.

Thermal Performance	Fission Gas Release	Dimensional Changes	Integral Effects
IFA-410 IFA-411 IFA-418 IFA-429 IFA-431 IFA-432 IFA-504 IFA-505 IFA-509 IFA-513 IFA-522 IFA-562	IFA-429 IFA-432 IFA-504 IFA-505 IFA-513 IFA-518 IFA-519	IFA-227 IFA-404 IFA-414 IFA-509 IFA-512 IFA-519 IFA-520 IFA-525	IFA-429 IFA-432 IFA-504 IFA-505 IFA-509 IFA-513 IFA-522 IFA-552 IFA-562.1

Thermal performance has been given the most attention in this report, and this is because it is recognised as *the* most important aspect of fuel behaviour to get right. The database is the most extensive and provides coverage of practically all the situations of interest. The table below gives experiments awarded the highest priority, but there is also a case for an analysis of the data to provide guidelines of common trends. In effect, such an exercise has already been performed for fission gas release, where the empirical relation between temperature and burnup provides a guideline for the onset of release in excess of 1%. For thermal performance, examples where common trends could be devised are: the dependence of temperature with gap dimension for helium and xenon fill rods at start-of-life, for the situation of closed gaps, the difference in temperatures between rods filled with helium and those filled with xenon, and finally, the trend of temperature versus burnup at constant

power levels. These serve as good starting points for model development and validation as they represent the databases as a whole.

Further steps to make the data accessible would be to provide materials properties and dimensions, irradiation histories and instrument measurements starting with the experiments in the table above and providing a commentary on further experiments which could be accessed and the means of doing so. It is recommended that data be assembled under the topics as presented in this report. The exception is high burnup data, and these could be packaged as presented in the table given in Table 6. All of the data considered in this report are available to Halden Project Participants and much of has been declassified for external use. Prior to assembling and releasing the data outside the Project, it must be established that all the data included in the databases are cleared for issue.

As mentioned in the introduction, irradiation histories and measurements are logged at 15 minute intervals. As a consequence, even for one experiment there are very many data points, and handling becomes a major part of the exercise in model development or code validation. Data condensation schemes are available, but these all pre-judge the important features of the irradiation. Halden staff have devised a condensation method which has been used successfully recently in the IAEA FUMEX code comparison exercise, Reference [61,62]. Here the data were compressed onto a series of 3.5 in floppy disks with full instructions on how they should be read. There were no difficulties experienced by any of the participants and therefore it is proposed that this method is adopted for the construction of databases.

Although every care is taken by Halden to provide accurate data, there are always uncertainties associated with any measurement. Sometimes the uncertainties are specific to the experiment in which case these need to be quantified. There are also more general uncertainties, particularly with reference to the irradiation histories. Under normal conditions, the uncertainty associated with power is taken as +/- 5%, but under circumstances where there have been instrument failures, this can be exceeded. In which case, where known, such additional uncertainties need identifying.

5.2 Extension to Include Data from Other Sources

In addition to The Halden Project, data are now available from certain Studsvik ramp test programmes in Sweden and from the Risø fission gas release projects in Denmark. These have already been shown to be compatible with and complement Halden data particularly in the areas of PCI/SCC failure and PIE of ramp tested fuel. Additional information from these projects are outlined below.

Since the early 1970's, a long series of bilateral and international fuel R & D projects primarily addressing the PCI/SCC failure phenomenon have been conducted under the management of Studsvik Nuclear. In these tests, fuel rods and rodlets were irradiated in a variety of reactors under prototypic conditions before being shipped to Studsvik and testing in the R2 reactor. These tests provide a very comprehensive data set on PCI failure propensity in BWR and PWR fuel under a variety of ramp conditions, and, for rods that survived ramping without failure, data are available for fission gas release. An overview of the projects which could be included in the database is given in Table 7 taken from a recent paper by Grounes, Reference [63].

The Risø National Laboratory in Denmark have carried out three irradiation programmes of slow ramp and hold tests, so called 'bump tests' to investigate fission gas release and fuel microstructure changes. The first project bump tested Halden irradiated IFA-148 fuel which achieved 27-35 MWd/kgU. There were 8 tests covering this burnup range and the measured fission gas release was between 3.94 to 13.42 %, Reference [64,65]. The second project bump tested fuel re-instrumented with pressure transducers pre-irradiated in Halden as IFA-161 and GE fuel irradiated in

the American Millstone BWR power reactor. The burnup range studied was 32 to 51 MWd/kgU for Halden fuel and 20 to 35 MWd/kgU for GE fuel and the fission gas released spanned 5.6 to 8.5 % for Halden fuel and 20.1 to 34.6 % for the GE fuel. The fuel was extensively examined in the hot cells and the fuel dimensions and structure before and after testing were reported, [66].

The third and final project bump tested fuel re-instrumented with both pressure transducers and new centreline thermocouples. The fuel was from: Halden IFA 161, 15 to 52 MWd/kgU, GE BWR fuel 23 to 45 MWd/kgU and ANF PWR fuel of 43 MWd/kgU burnup. The data from this project are particularly valuable because of the in-pile data on fuel temperatures and pressures as well as extensive PIE at Risø and TUI Karlsruhe. PIE included an optical study and EPMA of the Rim Region, see Reference [67]. Table 8 provides information on the test matrix and PIE measurements performed.

CHAPTER 6

CONCLUSION AND RECOMMENDATION

The report has reviewed the data on fuel performance that is available from The Halden Project from which it is possible to develop models describing the fundamentals of fuel performance. The report has reviewed the data under topic headings based on the basic phenomena affecting the behaviour of fuel and cladding during irradiation. Data available from other sources, in particular Studsvik Nuclear and the Risø Laboratories are mentioned briefly.

It is recommended that the international nuclear industry would benefit considerably by the assembly of a comprehensive database including the data reviewed here and datasets that are available from other sources. In this respect, attention should be paid to obtain data for reactor systems other than BWR and PWR, for example, WWER, CAGR and CANDU reactors. Models and codes which have a universal applicability independent of reactor system are much more robust than those benchmarked against a limited set of prototypic data, and as such, can be expected to provide reliable predictions outside the database from which they were developed.

The assembly of the database requires a substantial effort if it is to be accurate and easy to use. A tried and tested method of data transmission has been developed for the IAEA FUMEX code comparison exercise. This was found successful by code users from a wide variety of countries and therefore it is recommended that this method is employed for the proposed database.

It is recommended that the Halden experiments identified in section 5 should be the first to be included in the proposed database. These should be supplemented by data from the Risø projects and the Studsvik ramp programme where available for open distribution.

A future goal is the identification of additional data. Where ever possible data should be obtained to cover as many reactor systems as possible. The use of such diverse data assists in the development of mechanistic models which to be preferred to empirical correlations based on a limited dataset.

Finally, despite the comprehensive nature of the data available as outlined in this report, it is clear that there are a number of areas where further experiments are necessary. With the move to higher discharge burnup, it is necessary to extend the data to cover the extremes of burnup and power expected in commercial reactors. This implies a progressive extension of well qualified data in excess of 70 MWd/kgUO_2. New effects are being discovered at these levels of burnup and further data are required on such topics as: 'the rim effect', further definition of the effect of burnup on fuel thermal conductivity, clad corrosion and hydriding and clad mechanical properties. Although there are data on temperature changes during reactor scrams, for transient analysis, there is a need for data on the evolution of temperatures during rapid power changes. There are few data on this last topic and there is clearly a benefit to be claimed in reactivity faults for example, to exploit the lag between power increase and consequent increase in temperature.

Acknowledgements

The author wishes to thank the staff of The Halden Reactor Project, in particular, A. Hanevik, E. Kolstad and C. Vitanza for help during the preparation of this report.

References

Note: Halden Project publications in the HPR and HWR series which are less than five years old are available to Project Participants only.

[1] M. R. Smith, W. Wiesenack, H. Devold: "Review of Halden Tests and Measurements Relevant to Fuel Rod Thermal Properties". HWR-302 June 1991.

[2] N. T. Førdestrømmen, K. Haugset, T. C. Rowland, C. Vitanza: "Radial Power Distribution in HBWR-and LWR-Fuel Rods". HWR-75 June 1982.

[3] I. D. Palmer, K. W. Hesketh and P. A. Jackson: "Water Reactor Fuel Element Performance Computer Modelling". (J Gittus ed.) Applied Science, U.K. (1983) 321.

[4] C. O'Carrol, C. T. Walker and J. van de Laar, TUI and C. G. Ott, R. Restani, PSI: "Validation of the TUBRNP Model with the Radial Distribution of Plutonium in MOX Fuel Evaluation by SIMs and EPMA". Paper 2.9, IAEA Technical Meeting on Water Reactor Fuel Element Modelling at High Burnup and Experimental Support, 18-23 September, Windermere England.

[5] P. M. Crosby, C. Vitanza: "Irradiation of the Pellet Roughness Rig IFA-562.Progress Report March 1988". HWR-238 March 1988.

[6] F. Sontheimer: "Fuel Thermal Conductivity Changes with Burnup as Derived from In-Pile Temperature Measurements". HWR-299 June 1991.

[7] P. M. Crosby, E. Kolstad, T. Tsukada: "A Review of Thermal Feedback Effects in Fuel Rods of Different Designs and Irradiation Conditions". HWR-215 April 1987.

[8] D. O. Sheppard, C. Vitanza, H. Devold, K. Yanagisawa, D. Zorini: "Fission Gas Release: A Survey of Recent Experience at Halden". HPR-242 May 1980.

[9] T. Yagi, E. Kolstad: "Mechanical and Thermal Performance Data during Load Follow Operation. Preliminary Status Report on IFA-507 (HP)".
HPR-229 vol II paper 9 June 1979.

[10] D. Zorini, U. Graziani: "Status Report of the 3-Rod Diameter Rig IFA-509 (NUCLITAL/ HP)".
HPR-235 May 1980.

[11] T. J. Haste, J. A. Turnbull, D. Zorini: "A Study of Fuel Rod Thermal Behaviour Under Transient Conditions". HPR-276 May 1981.

[12] P. Lösönen: "Comparison of Burnup Dependent Steady-State and Dynamic Rod Thermal Response". HWR-249 January 1990

[13] W. Wiesenac: "An Assessment of Factors Affecting Stored Energy in Fuel Rods".
HWR-300 June 1991.

[14] H. Devold: “The Influence of Fuel Parameters on the Densification/Swelling Behaviour on Pellet Fuel up to 30 MWD/kgUO_2”. HWR-200 May 1988.

[15] H. Devold: “Characterisation of Swelling Rate of High Burnup Fuel (IFA-515)”. HWR-252 January 1990.

[16] I. D. Palmer, J. C. Killeen, E. Kolstad: “Equiaxed Grain Growth in UO_2, Assessment of Data from the HBWR”. HWR-164 March 1986.

[17] R. J. White: “Review of Fission Product Release Measurements from Fuel Irradiated in the Gas Flow Rigs, 1980-1985”. HPR-326 June 1985.

[18] J. Killeen, E. Skattum, A. Haaland: “IFA-504: Review of Fission Product Release Mechanisms and Thermal Behaviour Up to 30 MWd/kgUO_2”. HWR-231 April 1988.

[19] P. Wood: “Thermal Behaviour and Fission Product Release in the Gas-Flow Rig IFA-504 up to 50 MWd/kgUO_2”. HWR-332 January 1993.

[20] P. Tempest, E. Skattum, A. Haaland: “Fission Gas Release During Stepped Power Increases in the Gas Flow Rig IFA-558 above 15 MWd/kgUO_2”. HWR-258 January 1990.

[21] C. Vitanza, U. Graziani, N. T. Førdestrømmen and K. O. Vilpponen: “Fission Gas Release from In-Pile Pressure Measurements”. HPR-221, EHPG Loen 4-9 June 1978.

[22] M. E. Cunningham, K. Svanholm: “Fission Gas Release from PWR-Type Rods in IFA-429 during Rapid and Short Power Increases”. HWR-159 March 1986.

[23] M. R. Smith, P. M. Crosby, J. M. Aasgaard, Y. Minagawa: “Fission Gas Release During a Second Series of Rapid Power Increases on IFA-429 Rods at 40 GWd/TUO_2”. HWR-237 April 1988.

[24] S. Granata, E. Kolstad, I. D. Palmer, V. Tosi: “Re-Instrumentation Process Qualification for High Burnup Rods: Gas Pressure Detection and Fission Gas Release Evaluation during Power Ramps”. HWR-154 January 1986.

[25] V. Tosi, H. Amano: “Ramp Release in BWR Type Rods at High Burnup”. HWR-167 March 1986.

[26] V. Tosi: “The Effect of Pressurisation on Fission Gas Release on High Burnup BWR-type Fuel Rods (IFA-535.5-6)”. HWR-198 April 1987.

[27] R. Sairanen, C. Vitanza, S. Kelppe, K. Ranta-Puska: “Steady State Fission Gas Release from IFA-505 Data Evaluation and Comparison with Release Models”. HWR-157 January 1986

[28] D. O. Sheppard, C. Vitanza, S. Granata: “Steady State (IFA-402.3) and Subsequent Ramp Testing (IFA-512.7) of 3 Fuel Rods to Study Kinetics of Fission Gas Release”. HPR-298 April 1983.

[29] P. Crosby: “Rod Internal Pressure and Centre Temperature Measurements during Power Ramping in IFA-513”. HWR-195 May 1987.

[30] M. E. Cunningham: “Comparison of FGR Behaviour of Solid/Annular Pellet Fuel Rods (IFA-518 & 517)”. HWR-153 March 1986.

[31] H. Devold: “Comparative Study on Performance Aspects of Solid and Hollow Pellet Fuel Rods with Emphasis on Fission Gas Release at High Burnup”. HWR-303 June 1991.

[32] V. Tosi: “Fission Gas Release Measurements under Steady-State and Load Follow Operation to 55 MWd/kgUO_2 (IFA-519)”. HWR-304 June 1991.

[33] H. U. Staal, S Granata: “Load Following Experiment in IFA-512.7. Internal Rod Pressure and Cladding Deformation Behaviour during the First Two Sequences of Power Cycles”. HWR-124 May 1984.

[34] H. U. Staal: “Results from Power Cycling Experiments in IFA-512 and IFA-519”. HWR-192 January 1987.

[35] H. Amano, J. Nakamura, Y. Minagawa: “Results from the Power Ramp/Cycling Experiments in the LWR Ramp Rigs IFA-520/525”. HWR-150 March 1986.

[36] B. F. Conroy, J. R. Thompson, E. Hoshi, A. Haaland, J. Minagawa, K. Svanholm, E. Skattum: “Failure Threshold Calibrations in HBWR and Fission Gas Release Measurements by Re-Irradiation of Medium Burnup BWR Segments in IFA-534 and IFA-531”. HWR-161 February 1986.

[37] V. Tosi, A. Haaland: “Fission Gas Release Behaviour of PWR-Type Rods During Load-Follow Operation to 44 MWd/kgUO_2”. HWR-253 January 1990.

[38] K. O. Vilpponen, K. Yanagisawa, H. Tanaka, D. O. Sheppard: “A Study on Interaction and Relaxation”. HPR-246 May 1980.

[39] K. O. Vilpponen, M. Uchida, E. Kolstad, R. Miller, P. Hofgaard: “Mechanical Behaviour of Fuel Rods at High Burnup”. HPR-221.07 EHPG Loen 4-9 June 1978.

[40] E. Kolstad: “On EOL Pressure in PWR Rods and Zircaloy Primary Creep”. HWR-270 January 1990.

[41] H. U. Staal, P. Gunnerud, A. Haaland: “The IFA-516 In-Reactor SCC Test. Experimental Procedure and Results”. HWR-191 February 1987.

[42] J. A. Turnbull, J. J. Serna, K. Swanholm, E. Kolstad: “In-pile SCC Tests Carried out with IFA-567 and PIE of the Failed Rod Number 7”. HWR-384 June 1994.

[43] T. Tsukada, T. Johnsen, P. Gunnerud, K. Fjellestad, C. Vitanza: “Analysis of the Waterside Corrosion Experiment in IFA-560.2”. HWR-236 April 1988.

[44] T. Kido, K. Ranta-Puska: “Zircaloy Corrosion at High LiOH Concentrations under PWR Conditions (IFA-568.1 Final Report)”. HWR-333 October 1992.

[45] E. Kolstad, H. Devold, H. U. Staal, J. Nakamura, K. Hayashi: “Review of Test Results on Gap Closure Behaviour and Mechanical Interaction Effects in the HBWR”. HWR-89 May 1983.

[46] H. G. Walger, K. D. Knudsen, E. Rolstad, K. Svanholm, K. D. Olshausen, A. Hanevik: “A Parametric Study of the Influence of Important Fuel Design Parameters on the Elongation and Bamboo-Ridge Formation of Zr-2 Clad UO_2 Fuel Rods”. HPR-141 August 1971.

[47] V. Albergamo: “In-Pile Measurement of Cladding Length Changes in IFA-215 (HP)”. HPR-173 vol II. EHPG Sanderstølen, Norway, 19th to 23rd March 1973.

[48] OECD Halden Reactor Project Quarterly Progress Report, October to December 1973 HPR-167.

[49] H. U. Staal: “Radial and Axial Deformation Behaviour of Solid and Hollow Fuel Rods during Base Irradiation and Power Ramp in IFA-509.2”. HWR-49 May 1982.

[50] E. Kolstad: “The 3-Rod Diameter Rig Experiments IFA-404 I(HP) and IFA-404 II”. HPR-190 EHPG Geilo, Norway March 1975.

[51] S. Granata: “Data Analysis of IFA-402.3 Behaviour of Bellows Pressure Transducers”. HWR-72 June 1982.

[52] V. E. Hazel, S. de Carvalho, P. Hofgaard: “Cladding Elongation Measurements on 50 cm Long Fuel Rods in HBWR”. HPR-190 paper 25 EHPG Geilo, Norway March 1975.

[53] D. O. Sheppard: “Data Report IFA-507 from BOL to 15.4 MWd/kgUO_2”. HWR-74 June 1982.

[54] D. Zorini: “Mechanical and Thermal Performance of Fuel Rods in Load Cycling Operation. Status Report on IFA-507 (HP)”. HPR-236 May 1980.

[55] H. Devold, E. Kolstad, K. Svanholm, Y. Minagawa: “Dimensional Measurements on High Burnup BWR Rods up to > 40 MWd/UO_2 under Changing Power Conditions”. HWR-254 January 1990.

[56] M. Ichikawa, K. Yanagisawa, M. Fujita: “Influence of Base Irradiation of 17,000 MWd/tU on Cladding Diametral Deformation during Power Increase (IFA508/515,JAERI)”. HPR-286 EHPGM Hankø, Norway, 14th - 19th June 1981.

[57] U. Graziani: “Experimental Data Following an 85% Increase of the IFA-509 Assembly Power at 3800 MWd/tUO_2”. HPR-229 EHPG Hankø, Norway, 17th - 21st June 1979.

[58] C. B. Patterson, T. C. Rowland, L. D. Noble, J. S. Armijo: “Measurements of the Effects of Power Rates on Mechanical Interaction at Beginning of Irradiation”. HPR-229 vol III, EHPG Hankø, Norway, 17th - 21st June 1979.

[59] E. Kolstad: “Measurements of PCMI Deformations, Cladding Creepdown and Ovalisation Rates on the Fifth Rod in IFA-414 (IFA)”. HPR-211 paper 30 EHPG Loen, Norway, 4th - 9th June 1978.

[60] M. Uchida and M. Ichikawa: “In-pile Diameter Measurements of Light Water Reactor Test Fuel Rods for Assessment of Pellet Cladding Mechanical Interaction”. Nuclear Technology. 51 page 33 1980.

[61] P. Chantoin, J. A. Turnbull and W. Wiesenack: “Summary of the Findings of the FUMEX Programme”. Paper 1.1A, IAEA Technical Meeting on Water Reactor Fuel Element Modelling at High Burnup and Experimental Support, 18-23 September, Windermere England.

[62] W. Wiesenack: “Data for FUMEX: Results from Fuel Behaviour Studies at the OECD Halden Reactor Project for Model Validation and Development”. Paper 1.1B, IAEA Technical Meeting on Water Reactor Fuel Element Modelling at High Burnup and Experimental Support, 18-23 September, Windermere England.

[63] M. Grounes: “Studsvik's Fuel R & D Projects - A Review”. Paper 1.11, IAEA Technical Meeting on Water Reactor Fuel Element Modelling at High Burnup and Experimental Support, 18-23 September, Windermere England.

[64] P. Knudsen, C. Bagger, H. Carlsen, I. Misfeldt and M. Mogensen: “Data Report on the Risø Fission Gas Project”. Internal Report: Risø R511.

[65] M. Mogensen, C. T Walker, I. L. F. Ray and M Coquerelle: “Local Fission Gas Release and Swelling in Water Reactor Fuel during Slow Power Transients”. J. Nucl. Mater. 131, 162-171, 1985.

[66] Second Risø Fission Gas Release Project. Final Report, Risø Internal Document.

[67] Third Risø Fission Gas Release Project. Final Report, Risø Internal Document March 1991.

Table 1

List of IFAs and associated instrumentation

IFA	Owner	Access	NDs Va	NDs Co	TF	ET	EC	EF	PF	Comments
203	RNC	R	-	4	2		-	-	2	
206	PNC	R	4	-	2		4	2	-	
207	PNC	R	4	-	2		4	2	-	
208	JAERI	R	-	-	1		4	3	-	
211	JAERI	R	-	-	3		4	1	-	
223	JAERI	R	-	-	4		3	3	-	
224	JAERI	R	4	-	2		4	4	-	
226	NFS	A	8	-	4		6	-	5	
230	JAERI	R	-	-	1		4	3	-	
410.1	HIT/TOSH	R	8	-	3		8	-	-	
411.1	HIT/TOSH	R	7	-	1		5	3	-	
415.1	HP	A	4	-	2		-	-	-	
415.2	HP	A	4	-	2		-	-	-	
415.3	HP	A	4	-	2		-	-	-	
418.1	CE/KWU	R	5	-	3		-	3	6	
419.1	CE/KWU	R	5	-	1		-	2	6	
427	CE/KWU	R	5	-	5		-	3	4	
428	CE/KWU	R	12	-	24		-	-	-	
429.1	HP/NRC	A	9	1			-	-	9	movable absorber shields
429.2	HP/NRC	A	9	1			-	-	9	
429.3	HP/NRC	A	9	1			-	-	9	
429.4	HP/NRC	A	9	1			-	-	9	
430	HP/NRC	A	9	-	12		-	-	6	Gas flow rig
431	HP/NRC	A	6	1	12		6	-	3	
432.1	HP/NRC	A	6	1	11		6	-	3	
432.2	HP/NRC	A	6	1	11		6	-	3	
501.1	JA/HI/TO	R	6	-	12		-	-	12	
501.2	JA/HI/TO	R	6	-	12		-	-	12	
501.3	JA/HI/TO	R	6	-	9		-	-	12	
501.4	JA/HI/TO	R	6	-	9		-	-	12	
501.5	JA/HI/TO	R	6	-	9		-	-	12	
501.6	JA/HI/TO	R	6	-	9		-	-	12	
501.7	JA/HI/TO	A	6	-	2		-	-	12	
504	HP	A	9	1	8		-	-	8	Gas flow rig
505.1	HP	A	8	2	16		-	-	-	
505.2	HP	A	8	2	14		-	-	-	
505.3	HP	A	8	2	14		-	-	-	
505.4	HP	A	8	2	14		-	-	-	
505.5	HP	A	8	2	8		-	-	-	
507.1	HP	A	6	1	6		6	-	-	Movable absorber shields
507.2	HP	R	6	1	3		3	-	-	
508.1	JAERI	R	5	-	3		3	-	-	3 Diameter gauges
508.2	JAERI	R	5	-	1		3	-	-	
509.1	NUCL/HP	R	4	1	1		3	3	-	3 Diameter gauges
509.2	AGIP/HP		4	1	1		3	3	-	

Table 1 continued

IFA	Owner	Access	NDs Va	NDs Co	TF	ET	EC	EF	PF	Comments
510.1	JAERI/MHI	R	-	-	2		2	-	-	
510.2	JAERI/MHI	R	-	-	2		2	-	-	
510.3	JAERI/MHI	R	-	-	2		2	-	-	
511.1	HP	A	11	1	4		3	-	5	Coolant/clad T/Cs
511.2	HP	A	11	1	-		1	-	2	
513.1	HP/USNRC	A	8	1	12		6	-	6	
513.2	HP/USNRC	A	8	1	10		5	-	5	
513.3	HP/USNRC	A	8	1	8		4	-	4	
513.4	HP/USNRC	A	8	1	6		3	-	4	
514	JAERI/PNC	R	6	-	2		3	3	2	He-3 coils
517.1	HP/USNRC	A	6	1	3		3	-	1	
518.1	HP/USNRC	A	8	-	5		8	-	4	
519.1	JA/HI/TO	R	4	1	3		3	-	-	3 diameter gauges
520.1	JAERI/HP	R	7	1	1		1	1	-	2 diameter gauges
522.1	HP	A	6	-	1		-	-	-	Gap Meter, dia gauges
522.2	HP	A	6	-	1		-	-	-	
522.3	HP	A	6	-	1		-	-	-	
522.4	HP	A	6	-	1		-	-	-	
523.1	JAERI/HP	A	11	1	5		4	-	4	Coolant T/Cs
524.1	JAERI/HP	A	8	-	7		6	-	6	Coolant T/Cs
525.1	JAERI/HP	A	7	1	1		1	-	-	2 Diameter gauges
525.2	JAERI/HP	A	7	1	1		-	-	-	
525.3	JAERI/HP	A	7	1	1		-	-	-	
525.4	JAERI/HP	A	7	1	1		-	-	-	
525.5	JAERI/HP	A	7	1	1		-	-	-	
527.1	USNRC	A	8	1	12		6	-	6	
527.2	USNRC	A	8	1	10		5	-	5	
529	JAERI/PN	R	6	-	-		4	3	9	
530.1	JAERI/TO	R	14	-	3		-	-	-	Diameter gauge
530.2	JAERI/TO	R	14	-	3		-	-	-	
533.1	HP	A	3	-	1		8	-	-	
534.1	HP	A	7	-	1		8	-	-	
534.6	HP	A	7	-	1		7	-	-	
536	GE	R	5	-	6		-	3	6	
537	GE	R	5	-	6		-	3	6	
538	GE	R	5	-	6		-	3	6	
539.1	JA/MHI/NFI	R	10	-	6		-	2	2	
539.2	JA/MHI/NFI	R	9	-	6		-	2	2	
552	IFE/KWU	A	7	-	5		5	-	3	
553.1	FN/AGIP	R	6	-	3		-	-	12	
558	CEGB	A	7	1	12		-	-	6	Gas flow rig
559	JA/MHI/NFI	R	8	-	6		6	6	6	
561.1	JAERI/MHI	R	10	-	6		-	2	2	
562.1	HP	A	8	-	24		12	-	-	
562.2	HP	A	4	-	-	4	-	-	2	
563	HP	A	8	-	12		-	-	-	gas flushing
567	HP	A	6	-	4		-	-	-	SCC exp.
569	EPRI/NFIR	R	4	-	6		-	-	2	gas flushing

Table 2(a)

Small gap < 100 µm, helium filled high density fuel.

Access	IFA-	TF-No	Gap µm	Gas	Pressure Bar	Density % TD	Owner	Comment
A	415.1	1,2	70	He	1	96	HP	
A	431	5,6	50	He	1	95	HP/NRC	forerunner to IFA 432
A	432.1	4,5	80	He	1	95	HP/NRC	
R	501.1	8,10	70	He	3	95	J/HiT/Tosh	
R	501.5	11,	67	He	3	95	J/Hit/Tosh	
A	507.1	1,3,5	70	He	1	94	HP	
R	509.1	3,	60	He	1	95	Nuclital/HP	
R	519.1	1-3	70	He	3	95	J/Hit/Tosh	
A	524.1	3,4	80	He	32	95	J/HP	PWR conditions
A	525.1/2	1	80	He	32	95	J/HP	PWR conditions
R	536	1,3,5	76	He	10	97	GE	Low enriched 3.9%
R	537	1,3,5	76	He	10	97	GE	Low enriched 3.9%
R	538	1,3,5	76	He	10	97	GE	Low enriched 3.9%
A	562.1	5,6,11,12	55-76	He	1	96	HP	Low enriched 4% different roughnesses
A	562.1	17,18,23,24	71-12	He	1	96	HP	As above different vendor

Table 2(b)

Small gap < 100µm, xenon filled/contaminated high density fuel.

Access	IFA-No	TF-No	Gap µm	Gas	Press. Bar	Density % TD	Owner	Comments
A	505.1	9	50	23Xe/77He	1	95	HP	Small grain densifying fuel
A	505.1	10,13,16	50	Xe	1	95	HP	Small grain densifying fuel
A	505.1	1	50	Xe	1	95	HP	6% enriched
A	527.1	11,12	40	Xe	1	95	USNRC	
A	562.1	1-4	55-77	Xe	1	95	HP	low enriched 4% different roughnesses
A	562.1	7-10	55-77	Xe	1	95	HP	
A	562.1	13-16	71-71	Xe	1	95	HP	as above different vendor
A	562.1	19-22	71-72	Xe	1	95	HP	

Table 2(c)

Intermediate gaps, 100 < gap < 200 µm helium filled high density fuel.

Access	IFA-No.	TF-No.	Gap µm	Gas	Press. Bar	Density % TD	Owner	Comments
R	223	1-4	150	He	1	95	JAERI	
A	226	1	190	He	1	96	NFS	TFs 2 & 4 in 92% TD pellets
R	411.1	1	172	He	1	95	HIT/ Toshiba	
A	430	4,5	100	He	3	95	HP/ USNRC	sibling rod to gas flow rod
A	505.1	4	100	He	1	95	HP	Small grain densifying fuel
R	508.1	1,3	100	He	1	95	JAERI	
R	509.1	1	150	He	1	95	NUCLITAL/HP	Assembly contains other gap sizes
A	522.1	1	150	He	1	95	HP	Gap meter rig mechanical & free gap measured Xe filled rod in IFA-522.2
A	522.3	1	150	He	5	95	HP	
A	522.4	1	150	He	5	95	HP	
A	523.1	2,5	100	He	1	95	JAERI/HP	BWR loop & contitions
A	524.1	1,5,2 ,6,7	170	He	15-32	95	JAERI/HP	PWR loop and conditions Two different press. available
A	533.1	1	170	He	1	95	HP	Low enriched 2.4%
A	534.1	1	175	He	1	95	HP	Low enriched 3.5%
R	539.1L	2,3	170	He	1	95	JAERI/MHI/NFI	Assembly also contains Gd doped fuel
R	539.1U	5,3	170	He	1	95	JAERI/MHI/NFI	
A	552	2,5	130	He	10	94/95	IFE/KWU	Note high pressure
A	552	1,3,4	180	He	10	94/95	IFE/KWU	Note high pressure
R	559	7	170	He	10	95	JAERI/MHI/NFI	Assembly also contains MOX fuel
R	561	2,4,5 ,6,	170	He	1	95	JAERI/MHI	4 and 9% enriched Assembly also contains Gd doped fuel
R	562.2	1-4	100	He	10	94	HP	Thermal expansion thermometers

Table 2(d)

Intermediate gap, 100 < gap < 200µm, xenon filled/contaminated, high density fuel

Access	IFA-No	TF-No	Gap µm	Gas	Press. Bar	Density % TD	Owner	Comments
A	430	6	100	He/A/Xe	0-5	95	HP/ USNRC	gas flow rod
A	505.1	15	120	Xe	1	95	HP	Small grain densifying fuel
A	505.1	14	170	Xe	1	95	HP	
A	505.1	2,7	150	Xe	1	95	HP	
A	505.1	8,5,3,6	100	Xe	1	95	HP	
A	522.2	1	150	Xe	1	95	HP	gap meter rig He filled rods in other loadings
A	559	2	110	A	1	95	JAERI/ MHI/ NFI	assembly also contains MOX

Table 2(e)

Large gap > 200µm helium filled high density fuel

Access	IFA-No.	TF-No.	Gap µm	Gas	Pressure Bar	Density % TD	Owner	Comments
R	206	1,2	290	He	1	95	PNC	
R	207	1,2	290	He	1	96	PNC	
R	208	TF	300	He	1	95	JAERI	
R	230	2	250	He	1	95	JAERI	
R	410	1	400	He	1	95	Hit/Tosh	
R	410	2	300	He	1	95	Hit/Tosh	
R	410	3	200	He	1	95	Hit/Tosh	
R	418.1	1	230	He	35	96	CE/KWU	High pressure 6% enriched
R	418.1	2,3	310	He	22	96	CE/KWU	High pressure 2 enrichments
A	430	1,2,3	230	He	3	95	HP/USNRC	TF3 in gas flow rod
A	431	1,2,9-12	230	He	1	95	HP/USNRC	sibling to IFA-432
A	431	3,4	380	He	1	95		
A	432.1	1,2,8-11	230	He	1	95	HP/USNRC	
A	432.1	3,	380	He	1	95		
R	501	1-7	230	He	3	95	JAERI/Hit/ Toshiba	
A	504	1-8	200	He	1-40	95	HP	gas flow rig rod 3 with Nb doped fuel
A	505	11	220	He	1	95	HP	small grain densifying fuel
R	508	2	225	He	1	95	JAERI	
R	509.1	2	225	He	1	95	NUCLITAL/HP	
A	513.1	1-6,9,10	230	He	1	95	HP/USNRC	good for statistics
A	523.1	1	230	He	1	95	HP/JAERI	BWR conditions
R	536 537 538	2,4,6	203	He	10	96-97	GE	High pressure 3.9% enriched
R	553.1	2,3	200	He	5	95-97	FN/AGIP	
A	558	1-12	200	He	2-40	95	NE	gas flow rig different pressures
A	567	2,4	230	He	5	95	HP	SCC rig

Table 2(f)

Large gap > 200µm xenon filled/contaminated high density fuel

Access	IFA-No.	TF-No.	Gap µm	Gas	Press Bar	Density % TD	Owner	Comments
A	430	3	230	He/A/ (He/Xe)	1-5	95	HP/USNRC	gas flow rod
A	432.1	6,7	230	Xe	1	95	HP/USNRC	Constrained fuel stacks
A	504	1-8	200	He/A/Xe	1-40	95	HP	gas flow rig rod 3 with Nb doped fuel
A	505.1	12	200	Xe	1	95	HP	small grain densifying fuel
A	513.1	7,8	230	92%He/ 8%Xe	1	95	HP/USNRC	12 rods all with 230 µm gaps good for statistics
A	513.1	11,12	230	77%He/ 23%Xe	1	95		
A	527.1	1-10	230	Xe	1	95	USNRC	10 identical rods
A	567	1,3	230	Xe	1	95	HP	SCC exp.

Table 2(g)

Data from start-up ramps on fuel variants

A/R	IFA-No.	TF-No.	Gap µm	Gas	Pressure Bar	Density %TD	Variant	Owner	Comment
R	211	1-3	280	He	1	94	UO_2	JAERI	
R	224	1,2	300	He	1	90	UO_2	JAERI	
A	226	2,4 3	190 240	He	1	92	UO_2	NFS	TF-1 in 96% TD fuel pellets
R	419.1	1,2 3,4	230	He	22	91 94	UO_2	CE/KWU	
R	427	1,2,4 3,5	190 310	He	22	93	3.2% Pu UO_2	CE/KWU	TF-3 in rod at 35 bar
R	428	1,7 2,8,6 3,5,9,11 4,10,12 13,19,14,20 17,23 15,21,16,22 18,24	140 310 140 310 140 140 240 240	He/Xe He	22	93	UO_2 UO_2 UO_2 UO_2 3.2% Pu UO_2 3.2% Pu UO_2	CE/KWU	
A	429.1	1 2	200	He	25	93 91	UO_2	HP/ USNRC	
A	507.1	1,2	250	He	1	94	UO_2		
R	514	1,2	250	He	1	94	4.6% Pu	J/PNC	
A	517	1,2 3	260	He	5	92	Sph. pac UO_2	HP/ USNRC	
A	518	1 2,3 4,5	250	He	1	94/79 98/87 94	Vipac Vipac UO_2	USNRC	
R	529	1 2	190 320	He	1	94	6.2% Pu	J/PNC	
R	530	1,2 3	240	He	1	94 93	UO_2 6% Gd	J/Tosh	low enriched
R	539	1,4	170	He	1	95	6% Gd		
A	552	2 3	130 180	He	10	94		IFE/ KWU	
R	553.1	1	203	He	5	94		FN/AGIP	also 95 & 97 % TD rods
R	559	4,9 6,11	170 110	He A	10 1	95	6% Pu	J/MHI/ NFI	
R	561.1	1,3	170	He	1	95	10% Gd	J/MHI/ NFI	4% enriched
A	562.2	1-4	100	He	10	94		HP	Th Expansion Thermometer

Table 3

Through-life data of use to define the degradation of fuel conductivity with burnup

IFA-No.	Burnup	Rod No.	Gap	Gas	Typical Temperature
432 (phase 1,2,3,4)	0-35/1975-1984	3	70	1.0	800-1000
504 (He Flush phases)	0-35/1980-1990	1,3 4	200	= 1.5	650-950 and ramp to 1350
505	0-35/1978-1986	924D	100	1.0	850-1050 and ramp to 2050
507 (phase 1,2)	035/1977-1990	3	70	1.0	up to 1450
552	0-20/1984-1991	4,7 3,5,6	130 180	10.0	500-700
562.1	0-11/1987-1989	5,6,11,12	70	1.0	700-900 and ramp to 1450
562.2	0-25/1989-1992	16,17,18,19	100	10.0	900-1000

Table 4(a)

Fission gas data during rapid multiple power increases in the shield-lift experiment

Assembly	Rod No.	BU-oxide	fgr%-(meas.)
429	CB	32.7	17.28
-	CD	32.1	10.59
-	CH	35.0	20.29
-	AB	30.9	16.50
-	AD	31.5	16.45
-	AH	31.0	12.21

Table 4(b)

Fission gas release data available from reinstrumented pre-irradiated fuel rods

Assembly	Rod No.	BU-oxide	fgr%-(meas.)
535.2	08	34.8	24.0
-	-	-	64.0
535.3	509-3	28.7	7.7
-	-	-	23.0
535.4	211	-	17.0
-	-	-	24.0
-	212	-	3.0
-	-	-	fail
535.5	809	47.2	19.6
-	-	-	51.0
-	810	-	16.2
-	-	-	53.0
535.6	811	46.5	21.7
-	812	-	16.6
-	-	-	48.0

Table 5

Further details of a selection of experiments providing data on fission gas release under a variety of conditions

IFA	Owner	Access	Report	Rod no:	Design	Comment
429	HP	A	HWR-159 HWR-237 /22/,/23/	AB	91% TD fuel 17 µm grain size 200 µm gap 1 bar He	Rods base irr at ~20 kW/m to 30 MWd/kgUO_2. Fgr at end of base irr ~6-9% Rods subjected to series of rapid short duration transients: 15, 30, 60, 120 and 510 s. 3 rods in upper cluster failed after 4th transient. Fgr for lower rods ~17-35% 3 lower rods subjected to second set of similar transients at 40 MWd/kgUO_2. Fgr ~18-40%
				AD	93% TD fuel 17 µm grain size 200 µm gap 1 bar He	
				AH	95% TD fuel 17 µm grain size 200 µm gap 1 bar He	
				CB	95% TD fuel 5.9 µm grain size 200 µm gap 1 bar He	
				CD	95% TD fuel 17 µm grain size 200 µm gap 1 bar He	
				CH	95% TD fuel 17 µm grain size 360 µm gap 1 bar He	
432		A	HWR-215 /7/	1	95% TD fuel 230 µm gap 1 bar He	Good example of thermal feedback and effect on fuel temperatures in all but the low temperature rod 3.
				2	95% TD fuel 380 µm gap 1 bar He	
				3	95% TD fuel 76 µm gap 1 bar He	
				5	92% TD fuel 230 µm gap 1 bar He	
				6	92% TD fuel 230 µm gap 1 bar He	

Table 5 continued

IFA	Owner	Access	Report	Rod no:	Design	Comment
505	HP	A	HWR-157 /27/	26 short rods	Several different designs, gaps and fill gases	All rods equipped with thermocouples and fgr 0-30% measured by PIE. Burnup range 3-23 MWd/kgUO_2
IFA	Owner	Access	Report	Rod no:	Design	Comment
Base irr 402.3 Ramped in 512.7			HPR-298 /28/	6 rods	96.6% TD fuel 15-30 µm grain size 85 µm gap 1 bar He	Low power irr to 7 MWd/kgUO_2, 3 rods ramped to between40-51 kW/m and power cycled between 20-51 kW/m over 32 days. Fgr ~8-9%
513			HWR-195 /29/	1	230 µm gap 1 bar He	Ramped: rod 1 at 18 MWd/kgUO_2 to 45 kW/m rod 2 at 17.5 MWd/kgUO_2 to 47 kW/m rod 4 at 18.5 MWd/kgUO_2 to 44 kW/m
				2	230 µm gap 3 bar He	
				4	230 µm gap 92%He/8%Xe	
Base irr 518.1 Ramped in 517			HWR-153 /30/	R-5	solid pellet 8 µm grain size 250 µm gap 1 bar He	Rods equipped with PFs irradiated to 8- 9 MWd/kgUO_2 & ramped to 70 kW/m and held 8 hrs. Fgr was 4.7 & 4.1% in base & 40-46 & 40% after ramp in solid and hollow rods resp.
				AC-10	hollow pellet 8 µm grain size 250 µm gap 1 bar He	
518.2 518.3			HWR-303 /31/	R-24	solid pellet 8 µm grain size 256 µm gap 1 bar He	R-24 gave >10%fgr at 35 MWd/kgUO_2 after irr at 20-40 kW/m. ACP-28 gave 5-7% fgr at 52 MWd/kgUO_2 after irr at 20-40 kW/m. ACP-31 gave 2-2.5% fgr at 48 MWd/kgUO_2 after irr at 15-35 kW/m
				ACP-28 ACP-31	hollow pellets 8 µm grain size 270 µm gap 1 bar He	

Table 5 continued

IFA	Owner	Access	Report	Rod no:	Design	Comment
Base irr 429 Ramped in 519.9			HWR-304 /32/	DH	PWR rod 6 µm grain size 200 µm gap 25.9 bar He	Base irr at 20 kW/m in IFA 429 to 25-28 MWd/kgUO_2. Reloaded and operated at 40 kW/m and subjected to periodic load following, 20-40 kW/m; fgr was 20 and 25% for DH and DK resp.
				DK	PWR rod 17 µm grain size 360 µm gap 25.9 bar He	
Power cycling 512 519			HWR-124 HWR-192 /33/,/34/	402R5	15-20 µm grain size 85 µm gap 15.9 MWd/kgUO_2	Each rod subjected to 14 cycles: R5 29-45 kW/m R23 22-37 kW/m SP33 22-37 kW/m
				519-R23	solid pellet 260 µm gap 1 bar He 26.1 MWd/kgUO_2	
				519-SP33	Vib. compacted sphere pac 28.8 MWd/kgUO_2	
Base irr 523 Ramped in 520 PWR conditions in both rigs			HWR-150 /35/	PWR-13	95% TD fuel 176 µm gap 3.2 bar He	Base irr at <25 kW/m to 20 MWd/kgUO_2. Both rods ramped to 45 kW/m Rod 13 power cycled 621 cycles rod 14 held at constant 45 kW/m Fgr 18.6% and 18.4% for rods 13 & 14 resp.
				PWR-14	95% TD fuel 176 µm gap 3.2 bar He	
Base irr 524 Ramped in 520 BWR conditions in both rigs			HWR-150 /35/	4,5,6	95% TD fuel 230 µm gap 13.2-13.9 MWd/kgUO_2	Rods ramped to 45 kW/m and held constant whilst rod 6 was power cycled 30-45 kW/m thro 826 cycles in 13 days.
				11	106 µm gap 16.9 MWd/kgUO_2	
534.2			HWR-161 /36/	1,2	305 µm gap 3.1 bar He 9.3-13.9 MWd/kgUO_2	Rods ramped to 52 kW/m and held for >340 hrs Fgr: 24-28% rod 1 20-29% rod 2

Table 5 continued

IFA	Owner	Access	Report	Rod no:	Design	Comment
Re-inst HP rods Ramped in 535.1-.4			HWR-154 /24/	437-1	94.9% TD fuel 205 µm gap 9.0 MWd/kgUO_2	Rods were ramped to between46-52 kW/m. Rods 207 and 212 failed. Fgr ranged from 23 to 65%
				207	94.4% TD fuel 350 µm gap 35.8 MWd/kgUO_2	
				208	87.6% TD fuel 350 µm gap 35.8 MWd/kgUO_2	
				509.3	95% TD fuel 60 µm gap 28.9 MWd/kgUO_2	
553.1	FN/AGIP	R	HWR-253 /37/	12 rods	125 & 200 µm gap rods containing standard fuel and some containing fuel with different levels of additives.	Steady state irr at 25-30 kW/m to 35 MWd/kgUO_2

Table 6

Halden Project High Burnup Experiments

Experiment IFA-No.	Owner	Access	Burnup MWd/kgUO_2	Comments
408.3 408.4	IFE IFE	A A	54 54.6	Fuel swelling from stack elongation measurements
409.3 409.4	IFE IFE	A A	40.9 44.1	Fuel swelling from stack elongation measurements
416	ECN	R	42.6	Fuel and swelling measurements on fuel variants, eg. vibro.
429.7	HP	A	49.8	FGR (including power ramps ?)
504	HP	A	55.9	Gas flow rig for measuring radioactive FPR. Data on thermal performance through life with different gases in gap; gap dimension through hydraulic diameter measurement.
507.2	HP	A	41.8	Study of fuel temperatures, FGR and PCMI during power changes after prolonged low power operation.
512.11 512.12	HP HP	A A	42.3 45	To measure PCMI during load following
515.6 515.7 5.5.8 515.9	HP HP HP HP	A A A A	54.1 54.7 60.6 ?	.6-.8, Fuel swelling from stack length changes .9, measurement of ZrO_2 thermal conductivity by clad elongation
518.6	HP/NRC	A	66.4	Comparison of hollow and solid rods with emphasis on PCMI and FGR
519.9	HP	A	73.6	Investigation of effect of load following on FGR in PWR rods
533.2	HP	A	52	Re-instrumented rods for high burnup thermal performance
535.5 535.6	HP HP	A A	48 48.3	Investigation of effect of pre-pressurization on FGR under steady operating conditions
550.1 550.2 550.6 550.8	HP HP HP HP	A A A A	40.2 41.3 48.9 55.4	.1 .2 .6, Effect of load following on PCMI .8, ?
562.2 562.3 562.4	HP HP HP	A A A	50.1 62.7 76.3	Ultra high burnup experiment; will be unloaded at 80 MWd/kgUO_2. Contains solid rods and hollow rods with thermal expansion thermometers. Data on FGR and thermal performance.
565	JAERI/PNC	R	49.9	?
566.2 566.3 566.4	JAERI/NFD	R R R	44.3 42.2 41.2	FGR and swelling studies to high burnup
569.2 569.3 569.4	EPRI/ NFIR	R R R	32.9 52.1 67.7	Irradiation of fuel wafers for thermal conductivity studies during PIE

Access: A - available to Joint Programme Participants, R - restricted, permission required.

Table 7

Ramp Test Programme carried out by Studsvik Nuclear during 1975-93

Project (duration)	Fuel Type	No. of Rods	Base Irradiation (MWd/kgU)	Research Objectives
INTER-RAMP (1975-79)	BWR	20	Studsvik R2 (10-20)	Failure Threshold and mechanism, clad heat treatment.
OVER-RAMP (1977-80)	PWR	30	Obrigheim (10-30) BR-3 (15-25)	Failure threshold,design parameters.
DEMO-RAMP I (1979-82)	BWR	5	Ringhals I (15)	PCI remedy designs, annular pellet, Niobia dope fuel.
DEMO-RAMP II (1980-82)	BWR	8	Wurgassen (25-29)	Failure threshold, PCI damage by over power transients.
SUPER-RAMP (1980-83)	BWR	16	Wurgassen (30-35) Monticello (30)	Failure threshold, high burnup effects, PCI remedies, safe ramp rate, Gd fuel.
SUPER-RAMP	PWR	28	Obrigheim (33-45) BR-3 (28-33)	Effect of design parameters.
SUPER-RAMP EXTENSION (1984-86)	BWR	9	Oskarshamn 2 (27-31)	Safe ramp rate
SUPER-RAMP EXTENSION	PWR	4	Obrigheim (30-35)	Resolve unexplained failure resistance
TRANS-RAMP I (1982-84)	BWR	5	Wurgassen (18)	Determination of failure boundary, crack initiation and propagation, structural changes, fission gas release.
TRANS-RAMP II (1982-86)	PWR	7	Zorita (30)	Determination of failure boundary, crack initiation and propagation, structural changes, fission gas release.
SUPER-RAMP II 9x9 (1987-90)	BWR	4	Dresden (30)	PCI performance
ROPE I (1986-93)	BWR	4	Ringhals (36)	Investigate clad creep-out.
TRANS-RAMP IV (1989-94)	PWR	7	Gravelines (20-25)	Influence of non-penetrating cracks on PCI failure resistance.

Table 8(a)

Third Risø Fission Gas Release Project Test Matrix

Test	Type	Burnup % FIMA	Bump Power kW/m	Fill Gas	Hold time hours	Purpose
AN1	P	4.4	39.8	15 bar He	42	Effect of refabrication
AN2	U	4.3	39.0	25 bar He	62	Power history,effect of refabrication
AN3	TP	4.4	40.7	15 bar He	42	Fill gas, effect of refabrication
AN4	TP	4.4	40.7	1 bar Xe	42	Fill gas
AN8	U	4.3	29.8	25 bar He	4	Power history, fuel type, low power release
AN10	TP	4.4	34.4	5 bar He	40	Power history, low power release
AN11	U	4.4	16.9	25 bar He	4	Release at low power
GE2	TP	4.6	40.5	5 bar He	41	Burnup, power history
GE4	TP	2.4	43.3	5 bar He	34	Burnup, large grain size
GE6	TP	4.5	37.9	5 bar He	140	Power history
GE7	U	4.4	35.5	3 bar He	4	Power history, fuel type
II2	TP	2.8	42.8	5 bar He	2	Burnup, link to 2ond project
II3	TP	1.6	44.7	5 bar He	36	Burnup, link to 2ond project
II1	T	4.8	40.3	1 ba Xe	24	Link to 2ond project
II5	TP	5.3	40.1	5 bar He	24	Burnup, link to 2ond project

Note: P = pressure transducer, T = central thermocouple, U = unopened.

Table 8(b)

Hot Cell examinations

Non Destructive	**Observation**
Axial gamma scanning	Local relative power and burnup
Profilometry	Diameter change
Destructive examination	**Observation**
Puncturing	Analysis of released fission gases
X-ray fluorescence analysis (XRF)	Diametral Xe distribution (total gas content)
Electron probe micro analysis (EPMA)	Radial Xe content of matrix and small bubbles
Micro gamma scanning	Diametral ^{137}Cs distribution
Optical microscopy	Fuel structure
Replica electron microscopy	Distribution of bubbles >30 nm
Scanning electron microscopy	Fracture mode, grain boundary porosity
Transmission electron microscopy	Distribution of bubbles 1.5 to 30 nm
Burnup and heavy isotope analysis	determination as basis for fission gas generated
Retained gas measurement	Isotopic composition of retained fission gas

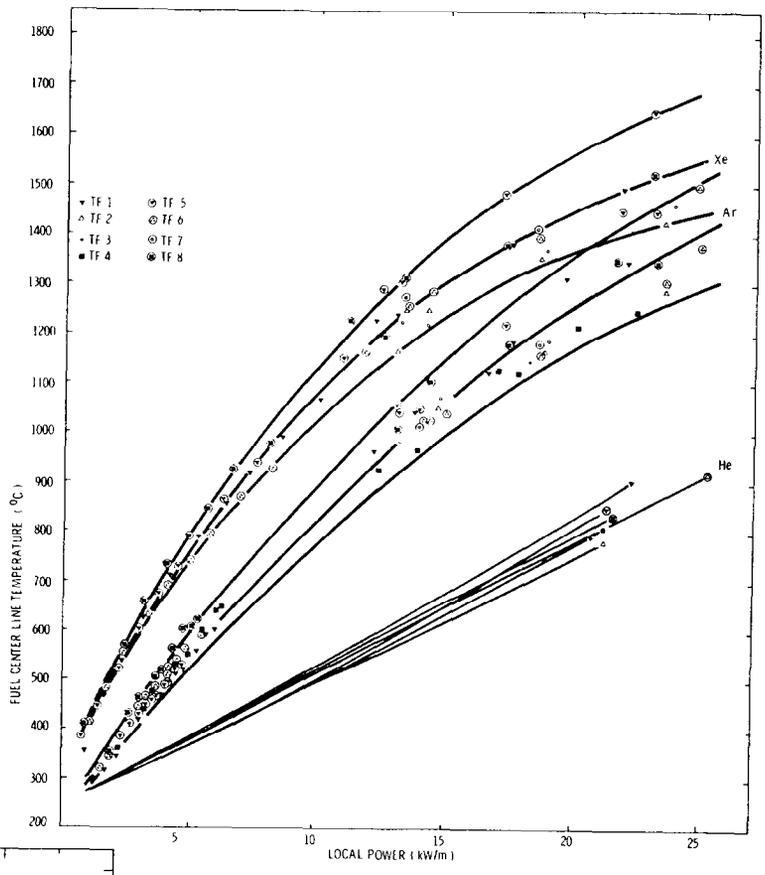

Figure 1

Fuel centreline temperatures recorded by all thermocouples for IFA-504 at beginning of life with helium, argon and xenon fill gas.

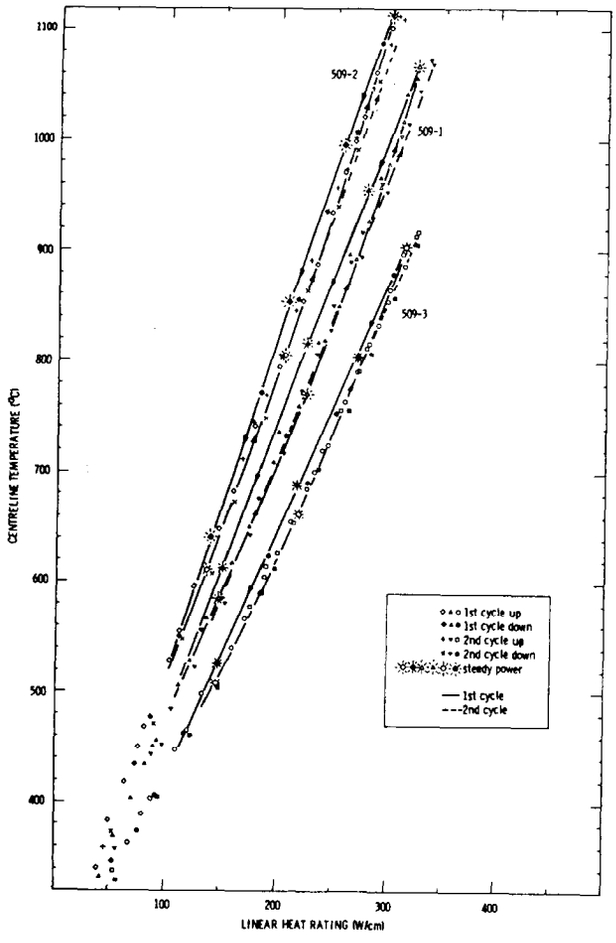

Figure 2

Centreline temperature versus local power for 3 rods of different gap size at the beginning of life for IFA-509.

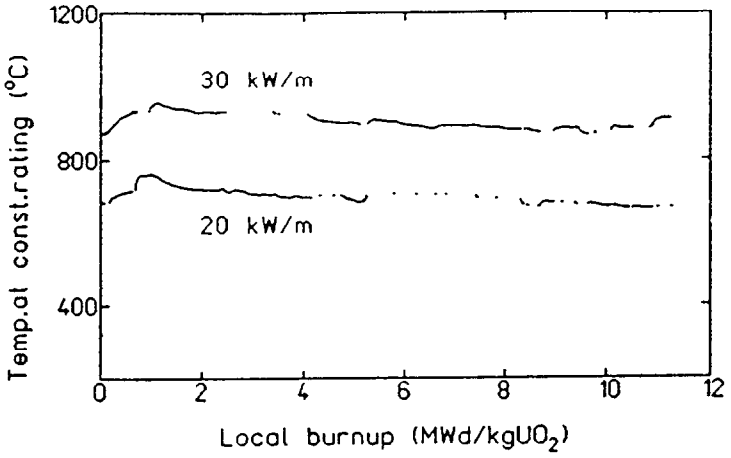

Figure 3(a)

Fuel centreline temperature normalized to 20 and 30 kW/m as a function of burn-up for the xenon filled rod 1 of IFA-562.1.

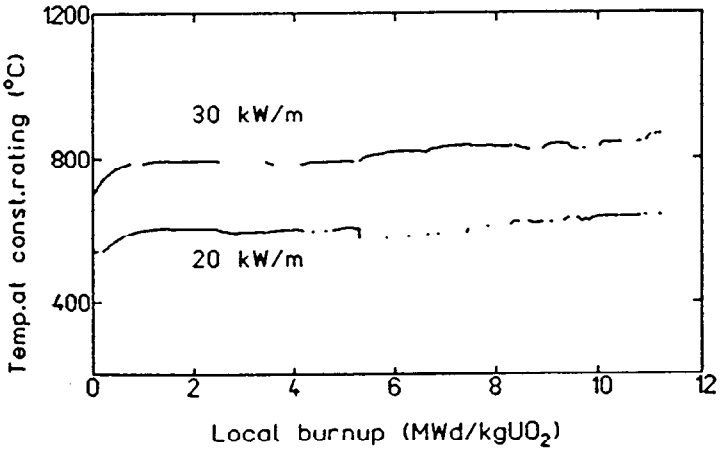

Figure 3(b)

Fuel centreline temperature normalized to 20 and 30 kW/m as a function of burn-up for the helium filled rod 11 of IFA-562.1.

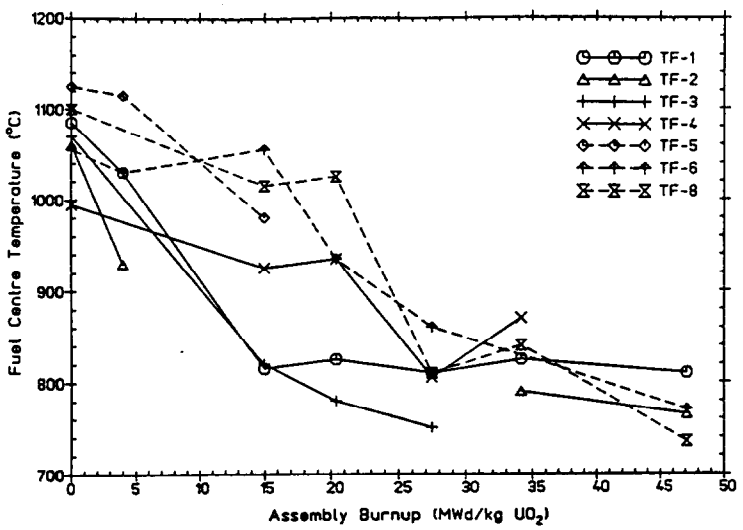

Figure 4(a)

Fuel centreline temperature normalized to 15 kW/m as a function of burn-up for the four rods of IFA-504 when filled with argon.

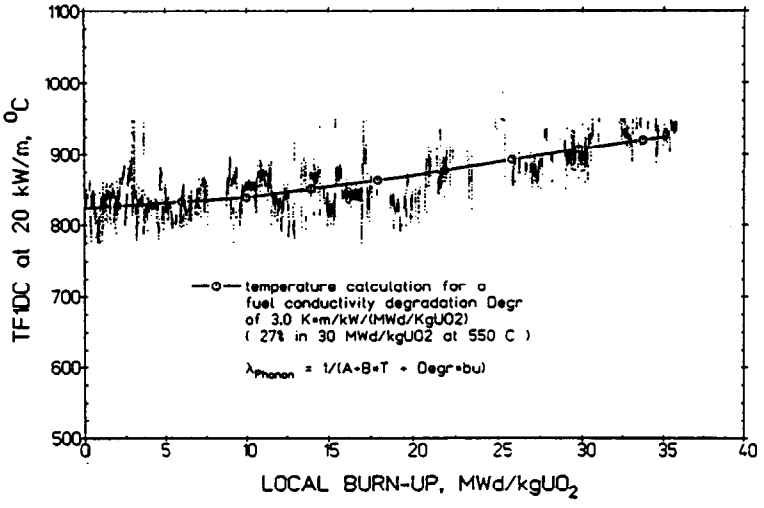

Figure 4(b)

Fuel centreline temperature normalized to 20 kW/m as a function of burn-up for the rod 1 of IFA-504 when filled with helium.

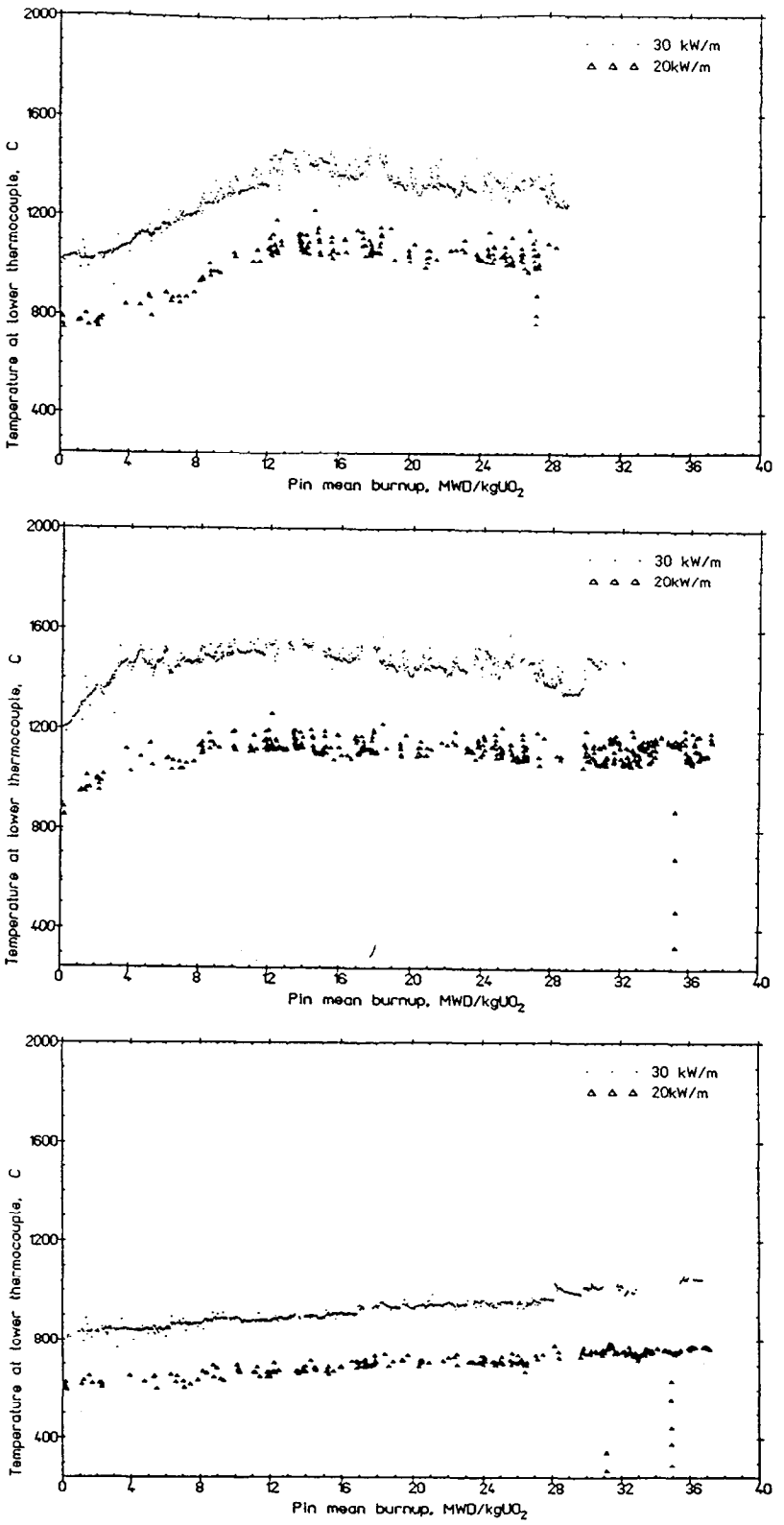

Figure 5(a-c)

Fuel centreline temperatures normalized to 20 and 30 kW/m plotted as a function of pin average burn-up for three rods with different gap sizes in IFA-432: (a) rod 1, 230 μm, (b) rod 2, 380 μm and (c) rod 3, 70 μm. (a) and (b) show the effect of fission gas release on fuel temperatures.

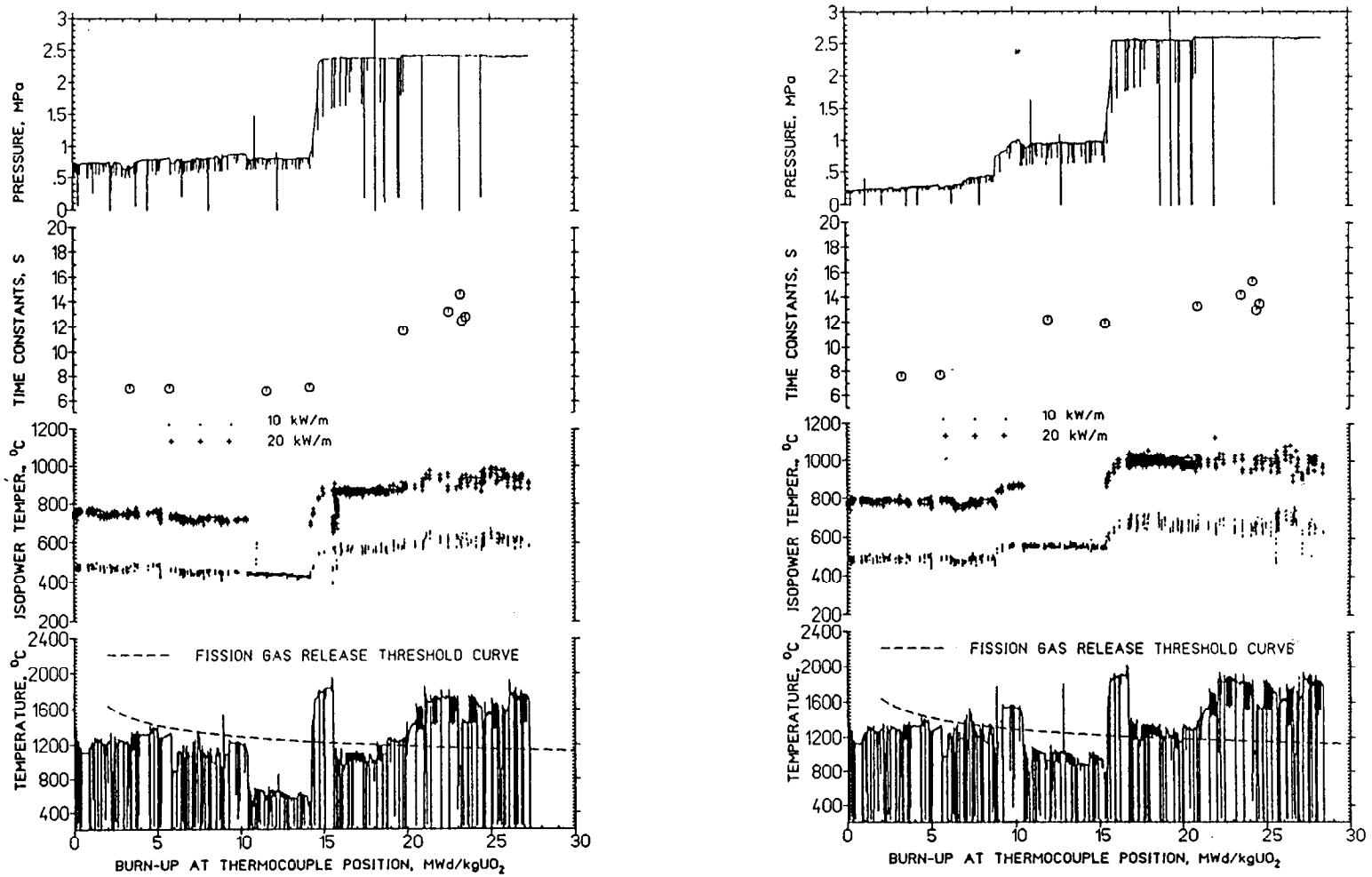

Figure 6

Data from rods 2 and 4 of IFA-513 showing the effect of fission gas release as indicated by rod pressure on fuel rod time constant and fuel centreline temperature normalized to 10 and 20 kW/m. The bottom graph shows the measured temperature throughout the history and the Halden empirical fission gas release threshold.

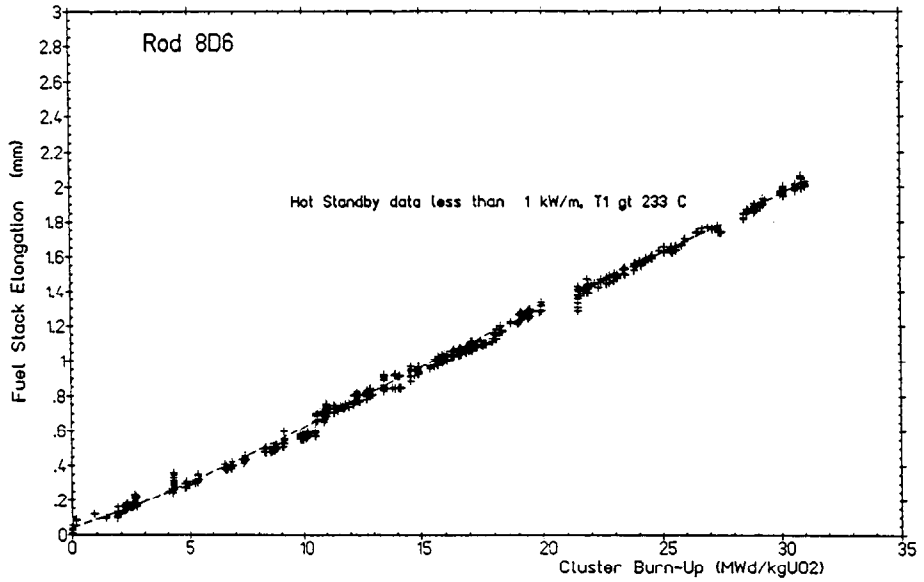

Figure 7

Fuel stack length measured at hot stand-by as a function of burn-up for rod 8D6 of IFA-408.2 showing the effect of solid fission product swelling.

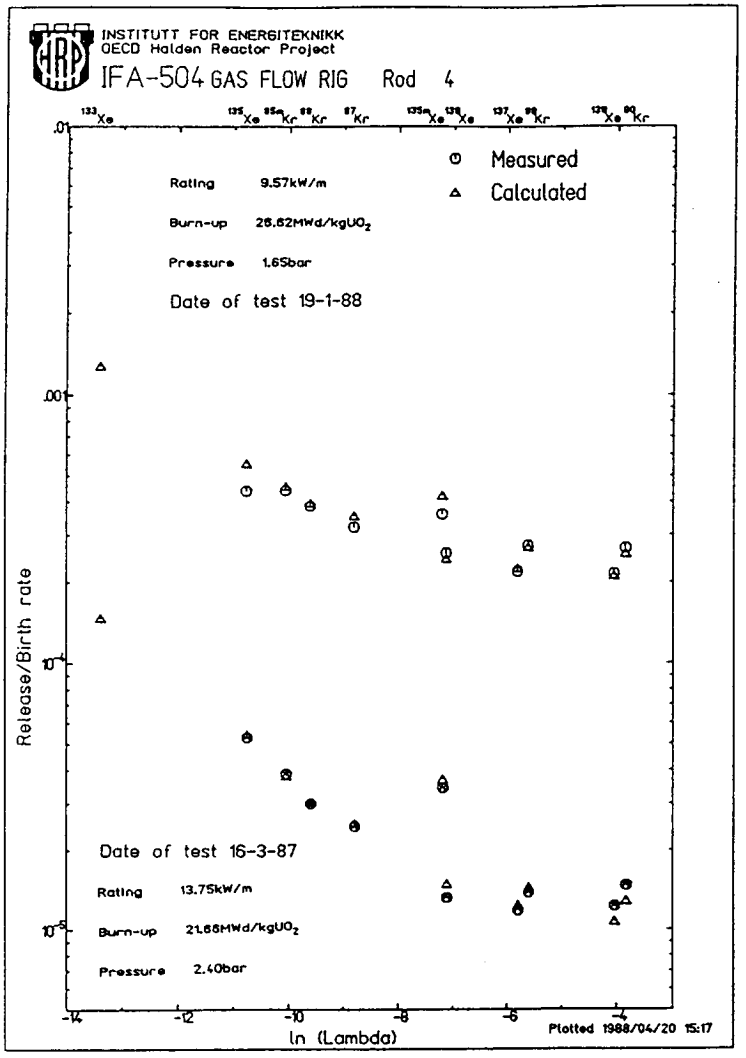

Figure 8

Plot of release to birth ratio (R/B), for the short lived fission gases in rod 4 of IFA-504 as a function of ln(λ). The $\lambda^{1/2}$ dependence of diffusive release is evident for the longer lived isotopes whilst the λ independent behaviour is evident for the shorter lived species. Data are presented before and after grain boundary interlinkage and show an identical form of behaviour.

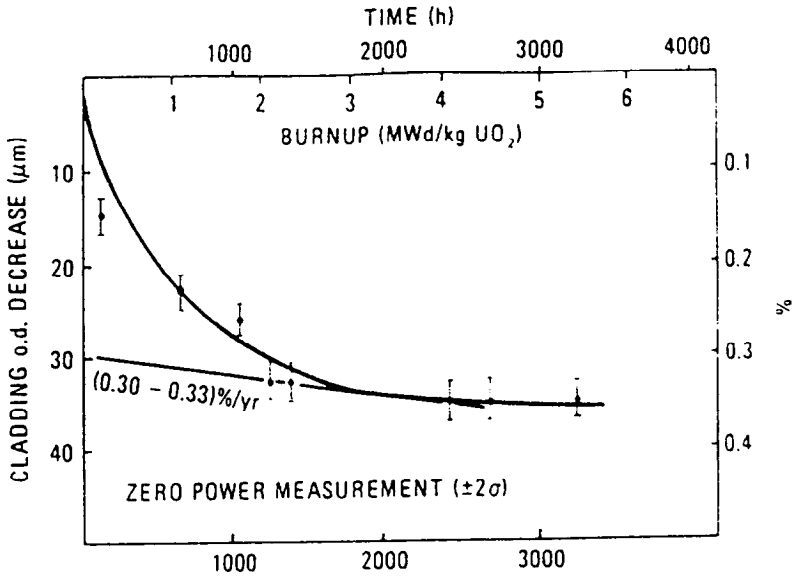

Figure 9

Measured Zircaloy-4 clad creepdown versus burn-up and time at power in the large gap segment of the 27 bar helium filled rod of IFA-414.

		INSTRUMENTS									DESIGN FEATURES		
IFA-no	MWd/kg/UO_2	Burnup	In reactor	Diameter gauges	Cladding extensometer	Fuel extensometer	Fuel thermocouple	Pressure sensor	Gap meter	He 3 coil	Solid absorber	Rotatable rods	In-core plug	Power ramping
116	3,5			•										
227	2,8		•	•										
401, 409	39/35	• •			•									
404	2,6		•	•										
414	5,4		•	•	•							•		
507	17	•		•		•					•			•
509	28	•	•	•	•	•								
504, 430	8/15	• •				•	•							
522	9,2	•	•	•		•		•	•				•	
512	8,6	•	•	•			•		•					•
436	1	•	•	•					•	•	•			•
508	25		•	•		•								
420	13,3	•	•	•					•					•
520, 525	6,7	• •	•	•		•	•		•		•			•

Figure 10

Instrumentation and design features of Halden mechanical interaction rigs.

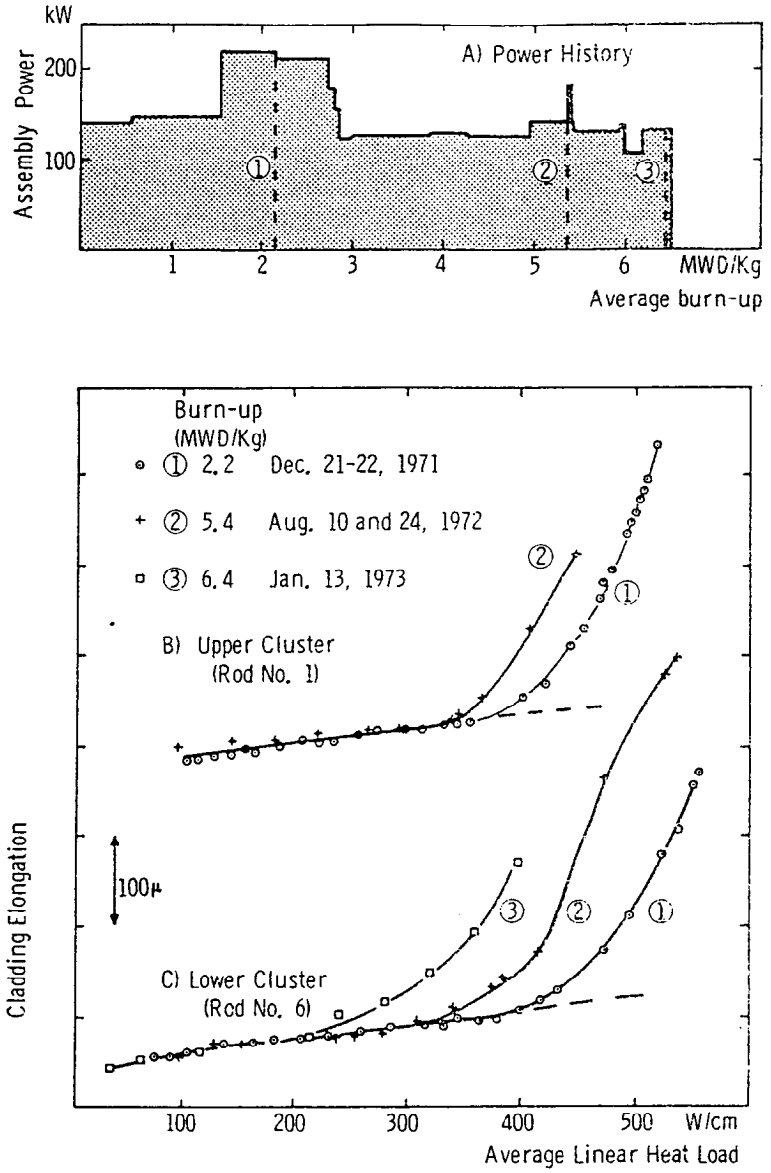

Figure 11

Clad elongation versus average linear heat rate during ramps at different occasions during irradiation of rods 1 and 6 of IFA-215 showing the effect of burn-up on the onset of mechanical interaction.

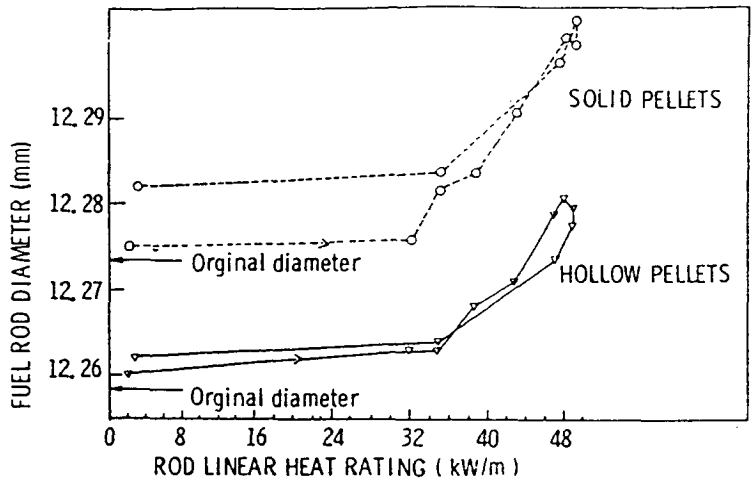

Figure 12

Clad average diameter versus linear heat rate for hollow and solid pellet rods in IFA-509 during a ramp at 3.0 MWd/kgUO_2. PCMI is much reduced in the hollow pellet rod and, unlike the solid pellet rod, results in no plastic permanent deformation of the clad.

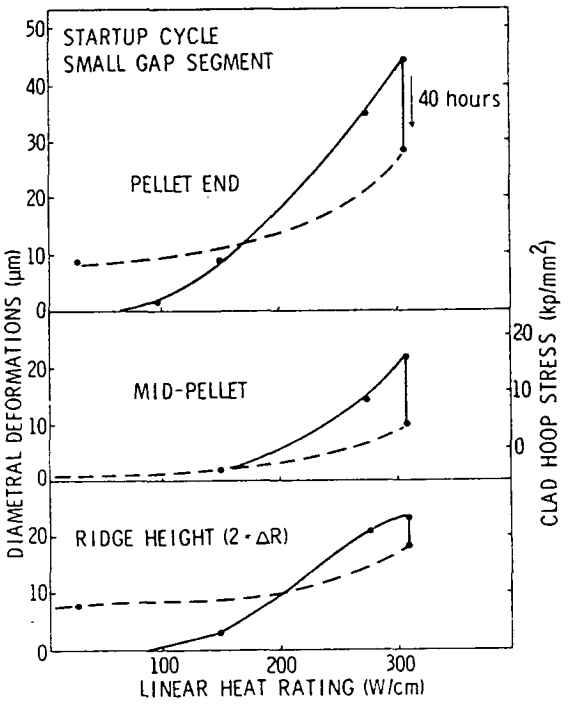

Figure 13

Measured deformations at pellet end and mid pellet positions in the small gap segment of IFA-414.5